Diadenosine-Polyphosphate Analogue AppCH2ppA Suppresses Seizures by Enhancing Adenosine Signaling in the Cortex

Alexandre Pons-Bennaceur, Vera Tsintsadze, Thi-Thien Bui, Timur Tsintsadze, Marat Minlebaev, Mathieu Milh, Didier Scavarda, Rashid Giniatullin, Raisa Giniatullin, Sergey Shityakov, et al.

Diadenosine-Polyphosphate Analogue AppCH2ppA Suppresses Seizures by Enhancing Adenosine Signaling in the Cortex

Alexandre Pons-Bennaceur, Vera Tsintsadze, Thi-Thien Bui, Timur Tsintsadze, Marat Minlebaev, Mathieu Milh, Didier Scavarda, Rashid Giniatullin, Raisa Giniatullin, Sergey Shityakov, et al.

Cerebral Cortex, 2018; 1–18

doi: 10.1093/cercor/bhy257
Original Article

ORIGINAL ARTICLE

Diadenosine-Polyphosphate Analogue $AppCH_2ppA$ Suppresses Seizures by Enhancing Adenosine Signaling in the Cortex

Alexandre Pons-Bennaceur[1], Vera Tsintsadze[1,2], Thi-thien Bui[3], Timur Tsintsadze[1], Marat Minlebaev[1,4], Mathieu Milh[5], Didier Scavarda[5], Rashid Giniatullin[4,6], Raisa Giniatullina[6], Sergey Shityakov[7], Michael Wright[8], Andrew D. Miller[8,9,10], Natalia Lozovaya[3] and Nail Burnashev[1]

[1]INSERM UMR1249, Mediterranean Institute of Neurobiology (INMED), Aix-Marseille University, Parc Scientifique de Luminy, BP13 Marseille, France, [2]Knight Cardiovascular Institute, Oregon Health and Science University, OR 97239, USA, [3]B&A Therapeutics, Ben-Ari Institute of Neuroarcheology, Batiment Beret-Delaage, Zone Luminy Biotech Entreprises, 13288 Marseille, Cedex 09, France, [4]Laboratory of Neurobiology, Kazan Federal University, Kazan 420008, Russia, [5]APHM, Department of Pediatric Neurosurgery and Neurology, CHU Timone, 13385 Marseille Cedex 5, France, [6]A.I. Virtanen Institute for Molecular Sciences, Department of Neurobiology, University of Eastern Finland, FI-70029 Kuopio, Finland, [7]Department of Anaesthesia and Critical Care, University of Würzburg, Josef-Schneider-Street 2, 97080 Würzburg, Germany, [8]School of Cancer and Pharmaceutical Sciences, King's College London, Franklin-Wilkins Building, Waterloo Campus, 150 Stamford Street, London SE1 9NH, UK, [9]Veterinary Research Institute, Hudcova 296/70, 62100 Brno, Czech Republic and [10]KP Therapeutics Ltd, 86 Deansgate, Manchester M3 2ER, UK

Address correspondence to Nail Burnashev and Natalia Lozovaya INMED, INSERM UMR1249, Parc scientifique de Luminy, 163 Avenue de Luminy, BP13-13273 Marseille Cedex 09, France. Email: nail.burnashev@inserm.fr (N.B.); lozovaya@neurochlore.fr (N.L.)

Abstract

Epilepsy is a multifactorial disorder associated with neuronal hyperexcitability that affects more than 1% of the human population. It has long been known that adenosine can reduce seizure generation in animal models of epilepsies. However, in addition to various side effects, the instability of adenosine has precluded its use as an anticonvulsant treatment. Here we report that a stable analogue of diadenosine-tetraphosphate: $AppCH_2ppA$ effectively suppresses spontaneous epileptiform activity in vitro and in vivo in a Tuberous Sclerosis Complex (TSC) mouse model ($Tsc1^{+/-}$), and in postsurgery cortical samples from TSC human patients. These effects are mediated by enhanced adenosine signaling in the cortex post local neuronal adenosine release. The released adenosine induces A1 receptor-dependent activation of potassium channels thereby reducing neuronal excitability, temporal summation, and hypersynchronicity. $AppCH_2ppA$ does not cause any disturbances of the main vital autonomous functions of $Tsc1^{+/-}$ mice in vivo. Therefore, we propose this compound to be a potent new candidate for adenosine-related treatment strategies to suppress intractable epilepsies.

Key words: adenosine, cortex, epilepsy, excitability, neurons

Introduction

About 1% of the world's population is affected by epileptic episodes during their lifetime, which makes epilepsy the second most frequent neurological disorder (Schmidt and Schachter 2014). Epilepsies are frequently described as an excitation/inhibition imbalance in neuronal network activity, that leads to synchronous and recurrent hyperactivation of large populations of neurons. Pharmacological antiepileptic treatments generally aim to restore the excitation/inhibition balance, either by activating inhibitory systems and/or by reducing excitatory drive. However, about 30–40% of epilepsies are pharmacoresistant (Sharma et al. 2015) highlighting the importance of developing novel therapeutic compounds focusing on new disease targets.

A large body of evidence shows that adenosine is an excellent candidate to block seizures in a variety of epileptic mouse models (Dunwiddie and Masino 2001; Huber et al. 2001; Boison 2005; Borea et al. 2016) including the temporal lobe epilepsy model (Hargus et al. 2012), the hyperthermia induced model (Leon-Navarro et al. 2015), and in the human surgical epileptic patient brain tissue (Angelatou et al. 1993). This anticonvulsant effect was shown primarily mediated by adenosine A1 receptor (A1R) activation (Gouder et al. 2003; Borea et al. 2016). Furthermore, A1R and adenosine levels rise locally as a consequence of epileptic crises and A1R antagonists have been shown to enhance the severity of seizures (Pagonopoulou et al. 2006; Amorim et al. 2016). Collectively these observations suggest that adenosine signals endogenous protective mechanisms to counteract epileptic seizures. Indeed, in animal models of chronic epilepsy as in human temporal lobe epilepsy, the basic levels of A1Rs are reduced, levels of adenosine kinase (ADK) (a main regulator of adenosine levels) are increased, and a low level of adenosine signaling appears to be a risk factor for seizure generation (Ault et al. 1987; Glass et al. 1996; Gouder et al. 2004; Boison 2006, 2012). However, utilization of adenosine as a pharmacological antiepileptic treatment is complicated by the rapid metabolism of adenosine by ADK (via phosphorylation). In addition, since adenosine plays a central role in regulation of important body functions such as temperature regulation or heart beating modulation, there is also concern that its usage might have severe side effects (Dunwiddie and Masino 2001; Boison 2005; Mustafa et al. 2009; Tupone et al. 2013; Li et al. 2016). Furthermore, the proconvulsant properties of A2A subtype adenosine receptors (A2ARs; as demonstrated in the pentylenetetrazol-induced kindled seizures model), have to be taken into account and have been suggested to limit utilization of adenosine as an antiepileptic drug (El Yacoubi et al. 2008, 2009).

For many years there has been an interest in diadenosine-polyphosphates (Ap_nA, where n is 2–7), as natural extracellular and intracellular signaling molecules present in the brain (Pintor et al. 1993; Baxi and Vishwanatha 1995; Miras-Portugal et al. 1999) that can regulate neuronal activity through activation of purinergic P2X and P2Y receptors (Pintor et al. 1993, 1996; Lazarowski et al. 1995; Pintor and Miras-Portugal 1995; Schachter et al. 1996; Wildman et al. 1999). We previously showed that a stable analogue of diadenosine-tetraphosphate, known as β, β′-methylene diadenosine 5′,5‴-P^1, P^4-tetraphosphate ($AppCH_2ppA$) selectively modulates the excitability of hippocampal CA1 pyramidal neurons (Melnik et al. 2006). We hypothesized that such a nonhydrolysable compound might exert targeted antiepileptic actions by an adenosine-dependent mechanism.

Now in order to test this hypothesis, we used a mouse model of Tuberous Sclerosis Complex (TSC). TSC is a rare genetic disease caused by inactivating mutations in *TSC1* or *TSC2* genes and the subsequent upregulation of the mammalian Target of Rapamycin (mTOR) pathway. The most frequent and devastating neurological symptoms of TSC are severe early pharmacoresistant epilepsies, affecting about 90% of the patients (Curatolo et al. 2008). The mTOR pathway is misregulated in several types of epilepsies, such as in cortical dysplasia or in temporal lobe epilepsies, and this is described to be (at least partially) responsible for the development of epileptic crises (Zeng et al. 2009; Meng et al. 2013; Lim et al. 2015; Moller et al. 2016; Marsan and Baulac 2018). Our recent study showed that heterozygote $Tsc1^{+/-}$ mice exhibit spontaneous epileptic seizures in vivo (Lozovaya et al. 2014) resembling those in human (Gataullina et al. 2016). In addition, somatic mutations in TSC1 and TSC2 have been proposed as a cause of focal cortical dysplasia (Lim et al. 2017). Thus, $Tsc1^{+/-}$ mice represent a good model for studying common mechanisms of epilepsy and for testing potential antiepileptic drugs. Here, we report that $AppCH_2ppA$ efficiently blocks epileptiform activities in an adenosine and A1R-dependent manner.

Materials and Methods

Animals

Breeding and experimental procedures were carried out in accordance with European guidelines for animal research, and in accordance with Institut National de la Santé et de la Recherche Médicale guidelines for animal care in research. All experiments were conducted in agreement with the European Directive 2010/63/EU requirements. Heterozygote $Tsc1^{+/-}$ (National Cancer Institute [NCI, USA]) male mice were kindly provided by Dr A. Bordey (Yale University, USA), with the genetic background B6;129S4-$Tsc1^{tm1.1Djk}$/Nci. This line of mice was generated by David J. Kwiatkowski (Brigham and Women's Hospital, Harvard Medical School, Cambridge, MA, USA). Inbred C57BL/6J wild-type ($Tsc1^{+/+}$) females were from Janvier Labs (France). Mice were housed in ventilated, light-tight, sound-isolated chambers under standard 12:12 light/dark cycle (light on at 07.00 PM and light off at 07.00 AM) with food and water available ad libitum. The genotyping of pups issuing from the cross-breeding of C57BL/6J $Tsc1^{+/-}$ male and C57BL/6J $Tsc1^{+/+}$ female mice was performed on tail tissue samples at postnatal day P9. The study was conducted in $Tsc1^{+/+}$ and $Tsc1^{+/-}$ mice of both sexes at P13-16. Pups from at least 3 deliveries for each condition were studied to minimize potential sampling bias.

Animal Slice Preparation

Mice at postnatal days P13–P15 were anaesthetized with ether and killed by decapitation. Transverse 300 µm thick coronal slices were cut using a vibratome (Leica VT1000S; Leica Microsystems Inc., Deerfield, IL, USA) in ice-cold protecting Choline solution containing (in mM): 118 choline chloride, 2.5 KCl, 0.7 $CaCl_2$, 7 $MgCl_2$, 1.2 NaH_2PO_4, 26 $NaHCO_3$ and 8 D-glucose; oxygenated with 95% O_2 and 5% of CO_2. Before recordings, slices were incubated in an artificial cerebrospinal fluid (ACSF-1) solution containing (in mM): 125 NaCl, 3.5 KCl, 0.7 $CaCl_2$, 3 $MgCl_2$, 1.25 NaH_2PO_4, 26 $NaHCO_3$ and 10 D-glucose (ACSF-1); equilibrated at pH 7.3 with 95% O_2 and 5% CO_2 at room temperature (20–23 °C) for at least 1 h to allow recovery. For the recordings, we used ACSF of the same composition but with 2 mM of $CaCl_2$ and 1 mM of $MgCl_2$ (ASCF-2).

Human Cortical Slice Preparation

After surgical resection, cortical tissue was placed within 30 s in an ice-cold oxygenated protecting solution that contained (in mM): 110 choline chloride, 26 $NaHCO_3$, 10 D-glucose, 11.6 sodium ascorbate, 7 $MgCl_2$, 3.1 sodium pyruvate, 2.5 KCl, 1.25 NaH_2PO_4 and 0.5 $CaCl_2$; 300 mOsm. Cortical slices (400–900 μm) were prepared in the same solution. The time gap between tissue collection and beginning of slice preparation was in the range of 10–15 min. After cutting, the slices were then transferred to holding chambers in which they were stored at room temperature (20–23 °C) in ACSF-1. Recordings were performed in ACSF-2.

Whole-Cell Recordings From Brain Slices

Slices were transferred to the recording chamber and superfused with oxygenated recording ACSF-2 at 3 mL/min. Neurons were visualized using infrared differential interference contrast (DIC) microscopy. Whole-cell patch clamp recordings were performed in layer 4 of the somatosensory cortex at room temperature by using either an EPC-9 amplifier and Patch Master software (HEKA Elektronik, Germany) or a Multiclamp 700B amplifier (Molecular Devices, Sunnyvale, CA, USA) with custom-made software based on IgorPro and filtered at 3–10 kHz. Patch pipettes were pulled from borosilicate glass capillaries (World Precision Instruments, Sarasota, USA) with 5–7 MΩ resistance when filled with the K-gluconate containing (Kglu) intracellular solution of the following composition (in mM): 130 K-gluconate, 10 Na-gluconate, 4 NaCl, 4 MgATP, 4 phosphocreatine, 10 HEPES and 0.3 GTP; pH 7.3 with KOH. Biocytin (final concentration of 0.3–0.5%) was added to the pipette solution to label the recorded neurons. Spontaneous excitatory postsynaptic currents (sEPSCs) were recorded in voltage clamp mode at −70 mV.

Evoked EPSCs (eEPSCs) and excitatory postsynaptic potentials (eEPSPs) were recorded in response to the extracellular stimulation of horizontal recurrent connections. A bipolar nickel/chromium electrode was positioned on the surface of the slice in layer 4 close to the recorded cells. Current pulses (10–100 μA) of 0.1–1 ms duration were delivered through the isolated stimulator (WPI, Sarasota, USA) at 0.05 Hz. The intensity of each stimulus was adjusted to <50% of maximum. A single pulse or a 50 Hz train of 5 stimuli were applied in tissue and both eEPSCs at −70 mV and eEPSPs at resting potentials were recorded. To estimate the kinetics of responses, for single eEPSPs, traces were normalized by peak amplitudes and the charge transfer of normalized responses was calculated. For the train eEPSPs the charge transfer was calculated for traces normalized by peak amplitudes after the last stimulus in the train. To estimate excitability of cells, voltage responses were recorded in a current clamp mode following injection of current steps of 1 s duration from −50 to 200 pA with an increment of 10 pA and 2 s intervals between each step. Current–voltage (*I*–*V*) relations were plotted from passives responses to estimate input resistance of the cells. Linear fitting of all cells *I*–*V* curves was performed and slopes of each curve were taken as an estimate of the mean membrane resistance.

Cell-Attached Recordings From Brain Slices

Single channel activities and spontaneous spiking were recorded in a cell-attached configuration with pipettes pulled to obtain resistance of approximately 10 MΩ. Single channel events were analyzed with Clampfit software under visual control. In some experiments the same cell was recorded simultaneously with 2 pipettes respectively filled with Kglu intracellular solution of previously described composition and cesium chloride containing solution (CsCl) with the following composition (in mM): 140 CsCl, 10 HEPES, 2 Mg-ATP, 0.3 GTP and 4 phosphocreatine; pH adjusted to 7.3 with CsOH.

Drugs

Compounds (10 μM of AppCH$_2$ppA), 10 μM of adenosine, 40 nM of 8-cyclopentyl-1,3-dipropylxanthine (DPCPX) (Tocris Bioscience, Bristol, UK), 10 μg/mL of adenosine deaminase (ADA) (Merck, Darmstadt, Germany), 100 μM of suramin hexasodium salt, 10 nM of MRS2500 tetraammonium salt (Tocris Bioscience, Bristol, UK), 100 nM of tertiapin-Q (Tocris Bioscience, Bristol, UK), 100 μM of adenosine 5′-(α,β-methylene) diphosphate (ADP-methylene) (Merck, Darmstadt, Germany) and 500 μM of bupivacaine were added to ACSF-2 and superfused with the same rate as control solution. Inosine (Merck, Darmstadt, Germany) at concentration of 100 μM was added to Kglu intracellular solution.

Analysis and Statistics of In Vitro Data

sEPSCs were analyzed using Mini Analysis 6.0.3 software (Synaptosoft Inc., Decatur, GA, USA). The threshold amplitude for detecting sEPSCs was set around 3 pA at twice the baseline noise (mean square root), and sEPSCs detected by the software were visually inspected to minimize errors. Events that did not show a typical synaptic waveform were rejected manually. Epileptiform bursts were defined as responses with at least 4 consecutive sEPSCs associated with a baseline elevation with the largest amplitude of the response ≥10 pA. Strengths of bursts were estimated by measurement of a single burst charge transfer (absolute area under the burst), maximal amplitude and total duration. Means of 20 bursts by condition and by cell were taken randomly to calculate averages. The eEPSCs and eEPSPs means were calculated from 10 averaged stimulation traces per cells and condition.

All data were further analyzed with Origin software (MicroCal, Northampton, MA, USA) and GraphPad Prism (GraphPad, La Jolla, USA). Data are expressed as mean±SEM. The normality of sample distributions was tested with the Kolmogorov–Smirnov normality test and paired sample *t*-tests were used for comparisons with threshold of $P < 0.05$. When data sample distributions were not normal the Wilcoxon test was used. Classical representation with stars was applied to show the *P*-values: $^{*}P < 0.05$; $^{**}P < 0.01$; $^{***}P < 0.001$. Detailed statistics and statistical tests for each experiment are provided in Supplementary Table S1.

In Vivo Recordings and Data Analysis

Experiments were performed on postnatal days P14–P16 of both sexes of *Tsc1*$^{+/-}$ mice. Mice were randomly picked from cage and genotyped after experiments. Surgery was performed under isoflurane anesthesia and lidocaine analgesia. During recordings, the head was fixed to the frame of a stereotaxic apparatus by attached bars; animals were surrounded by a cotton nest and heated via a thermal pad (36.6–37.7 °C). A silver chloride reference electrode was placed in the cerebellum or the visual cortex. EEG recordings were performed with nonanaesthetized head-restrained *Tsc1*$^{+/-}$ and control *Tsc1*$^{+/+}$ mice. A 16 site linear silicon probe (100 μm separation distance between recording sites, Neuronexus Technologies, MI, USA) was placed into the somatosensory cortex using the Paxinos and Franklin atlas (2001) at coordinates: anterior–posterior = 2–2.5 mm,

mediolateral = 2–3 mm from Bregma, 1.2–1.5 mm depth, in order to trace the columnar activity at all layers. Signals were amplified (×100) and filtered at 3 kHz using a 16-channel amplifier (A-M systems, Inc.), digitized at 10 kHz and then saved to the hard disk of a PC using the Axoscope software (Molecular Devices). Recordings were analyzed offline using Clampfit and MATLAB software (The Mathworks, Natick, MA, USA). After recording, the position of the silicone probe was verified visually by DiI staining of the electrode in 100 μm coronal sections from the fixed brain. We considered that multiunit activity occurred in epileptic discharges if they appeared in a group of multiple spikes whose amplitude exceeded at least twice the background activity within a period lasting for at least 20 s. During EEG recordings, animals were monitored visually to determine behavioral correlates of each electrographic epileptic discharge. During some recordings, AppCH$_2$ppA was intraperitoneally injected with dosages of 25 and 83 mg/kg to investigate its acute effects on in vivo epileptic crises. The first dosage did not abolish the occurrence of seizures but decreased their amplitude and duration, whereas the second was sufficient to completely block the crises. Thus, the 83 mg/kg dose was used for further analysis.

Measurements of the Main Vital Autonomous Functions

To assess the potential consequences of AppCH$_2$ppA administration on the general health of the treated *Tsc1*$^{+/-}$ mice, we measured weight before (W0), 1 h (W1), 3 h (W3), 24 h (W24) and 48 h (W48) after AppCH$_2$ppA i.p. injections. Body temperatures of mice were recorded using a rectal probe designed for small rodents before (T0), 1 h (T1), 3 h (T3), 24 h (T24) and 48 h (T48) after the injection. The heartbeat rates of mice were estimated using a piezo electrode placed on the thoracic area of the animal during EEG recordings. The frequencies of heartbeats were measured from 10 min traces before and 1 h after AppCH$_2$ppA injection. All the parameters were then compared with those of untreated control *Tsc1*$^{+/-}$ animals of the same age, from the same litter, also kept in the same conditions.

Human Subjects

Cortical tissue samples were obtained from 2 TSC epileptic patients undergoing surgery at the Departments of Pediatric Neurosurgery of Hopital La Timone (Marseille). Informed consent for the use of postsurgical tissue for research purposes was obtained with protocols approved by Hopital La Timone review boards. Personal data were stored in a specific database, which is declared to the Commission nationale de l'informatique et des libertés (CNIL). The main clinical and neuropathological characteristics of the study population are summarized in Supplementary Table S1. The study was proposed and performed with 2 TSC patients that underwent epilepsy surgery between January 2015 and June 2017.

Results

AppCH$_2$ppA Reduces Epileptiform Activity in *Tsc1*$^{+/-}$ Neocortical Slices

We have recently shown that sEPSCs recorded in neocortical excitatory neurons in brain slices from heterozygous *Tsc1*$^{+/-}$ mice, appear as repetitive, highly synchronized epileptiform bursts initiated in layer 4 spiny stellate cells (SSCs) (Lozovaya et al. 2014). Therefore, we performed voltage clamp whole-cell recordings of sEPSCs in somatosensory cortex layer 4 SSCs at −70 mV to test whether AppCH$_2$ppA would affect this epileptiform activity. Bath administration of 10 μM AppCH$_2$ppA significantly and reversibly reduced the frequency of bursts to 0.28 ± 0.08 of control (n = 12 cells, Wilcoxon test, P = 0.0010; 1.43 ± 0.27 after washout, n = 11 cells, Wilcoxon test, P = 0.0001) and abolished burst synchronicity (Fig. 1*A*,*B*,*D*). Accordingly, in current clamp whole-cell recordings the spontaneous spiking activity observed in SSCs of *Tsc1*$^{+/-}$ mice was totally abolished by the administration of AppCH$_2$ppA (Fig. 1*C*). AppCH$_2$ppA application also significantly reduced charge transfer by individual bursts to 0.60 ± 0.12 of control (n = 86 bursts, Wilcoxon test, P = 0.0122) by decreasing the total duration of bursts (393.7 ± 18.8 ms under control conditions to 184.2 ± 17.9 ms in the presence of AppCH$_2$ppA, paired sample t-test, P = 0.0000012) with maximal burst amplitudes being essentially unaltered (54.1 ± 5.6 pA under control conditions and 46.4 ± 7.1 pA in the presence of AppCH$_2$ppA, paired sample t-test, P = 0.44, Fig. 1*E*,*F*). Therefore, AppCH$_2$ppA exerts strong antiepileptic actions in *Tsc1*$^{+/-}$ mice in vitro. AppCH$_2$ppA administration also significantly and reversibly reduced the frequency of basal sEPSCs to 0.54 ± 0.08 of control (n = 9 cells, Wilcoxon test, P = 0.0005; 1.13 ± 0.12 after washout, n = 8 cells, Wilcoxon test, P = 0.0007, Fig. 1*G*, *H*). It is notable that, application of AppCH$_2$ppA produced an outward shift of 11.9 ± 1.4 pA (n = 13 cells) in a holding whole-cell current (ΔI) that completely disappeared after washout (Fig. 1*A*).

Antiepileptic Effects of AppCH$_2$ppA are Mediated by the Enhancement of Adenosine Signaling through A1 Receptors

To test the involvement of adenosine A1Rs in diadenosine polyphosphate-mediated antiepileptic effects (Klishin et al. 1994; Rubino and Burnstock 1996), we recorded sEPSCs in *Tsc1*$^{+/-}$ mice in the presence of the selective A1R antagonist DPCPX. Bath administration of 40 nM of DPCPX alone to the slices in *Tsc1*$^{+/-}$ mice did not change the level of sEPSC activity in layer 4 SSCs suggesting no drastic contribution of A1Rs to the basal activity level in these cells (presumably due to a low tonic adenosine level; Supplementary Fig. S1). The administration of 10 μM of AppCH$_2$ppA in the presence of 40 nM DPCPX did not alter burst frequency (1.23 ± 0.22 of control, n = 5 cells, Wilcoxon test, P = 0.3645, Fig. 1*D*), burst charge transfer (4.58 ± 1.54 pC under control conditions, 4.96 ± 2.67 pC in the presence of AppCH$_2$ppA, n = 200 bursts, P = 0.91) or the frequency of individual basal sEPSCs (1.27 ± 0.26 of control, n = 5 cells, Wilcoxon test, P = 0.3551, Fig. 1*H*). Therefore, AppCH$_2$ppA mediates all its actions on basal and paroxysmal activities in slices through the activation of A1Rs. To test whether activation of A1Rs was due to an increase in adenosine levels, we prevented extracellular adenosine accumulation using 10 μg/mL of ADA that irreversibly deaminates adenosine to inosine. Under these conditions, AppCH$_2$ppA did not exhibit antiepileptic effects either on burst frequency (0.77 ± 0.10 of control, n = 3 cells, Wilcoxon test, P = 0.250, Fig. 1*D*) or on sEPSC frequency (1.03 ± 0.05 of control, n = 5 cells, paired t-test, P = 0.599, Fig. 1*H*). This indicates that AppCH$_2$ppA induced antiepileptic effects are mediated in an adenosine- and A1R-dependent manner.

AppCH$_2$ppA Reduces Excitability of Layer 4 SSCs in *Tsc1*$^{+/-}$ mice

To further understand the antiepileptic mechanisms of AppCH$_2$ppA, we tested whether or not the intrinsic electrophysiological properties of the layer 4 SSCs in *Tsc1*$^{+/-}$ mice might be affected

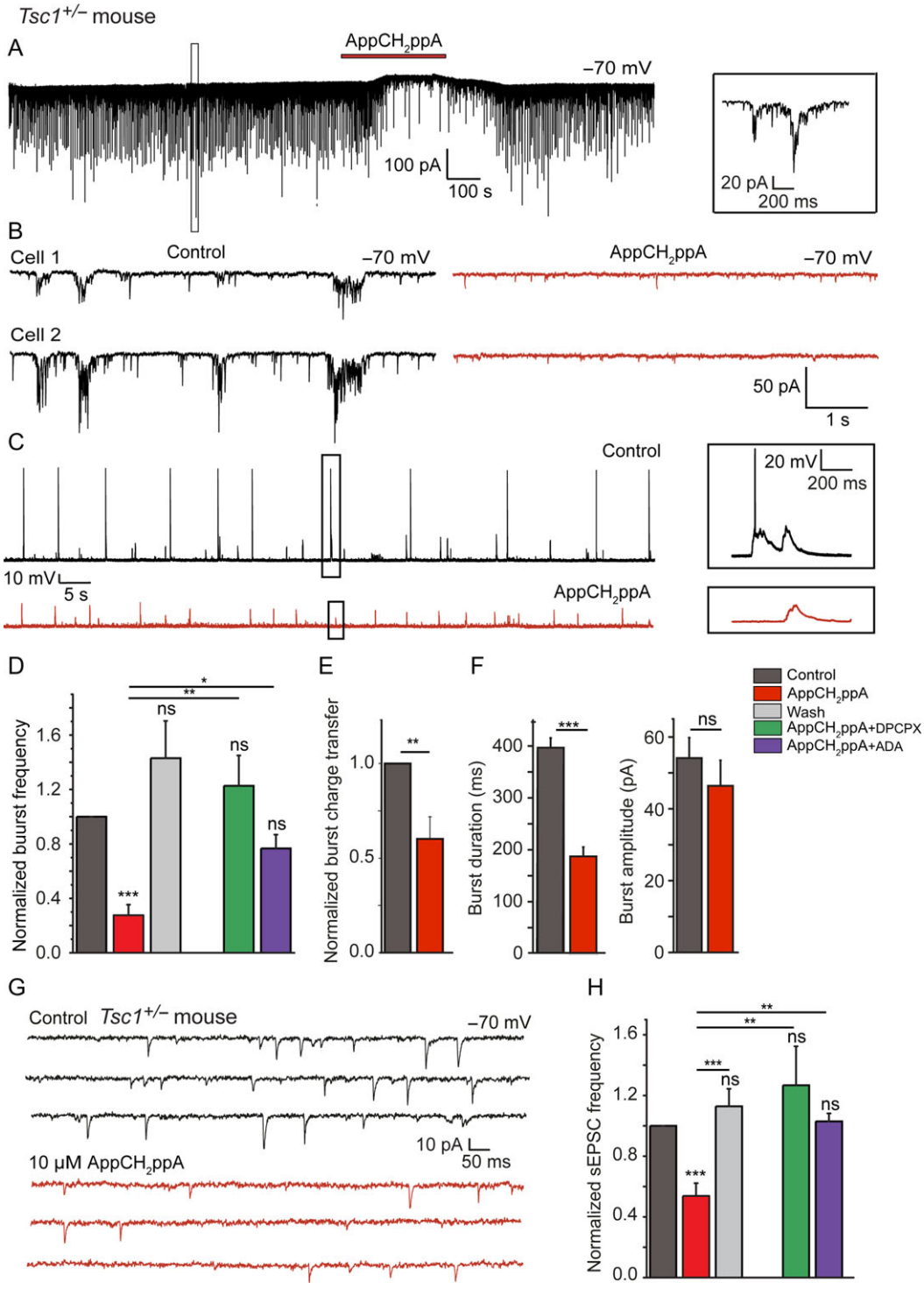

Figure 1. AppCH$_2$ppA strongly reduces the epileptiform activity in neocortical neurons in brain slices from *Tsc1*$^{+/-}$ mice. (*A*) Representative trace of whole-cell spontaneous epileptiform activity recorded from layer 4 SSCs in voltage clamp at –70 mV before and after bath application of AppCH$_2$ppA (10 µM). Inset on the right shows expanded trace of the bursts in box. (*B*) Representative traces recorded simultaneously from 2 SSCs in control condition (black traces) and in the presence of 10 µM of AppCH$_2$ppA (red traces). (*C*) Representative recordings of spontaneous potential firing in current clamp in SSC before (black trace) and after bath application of 10 µM AppCH$_2$ppA (red trace). Insets on the right show expanded traces of the potentials marked in boxes. (*D*) Summary data of the current bursts frequencies. (*E*) Summary data of bursts charge transfers. (*F*) Summary data of total duration (left) and maximal amplitude (right) of the current bursts. (*G*) Representative traces of interburst sEPSCs of layer 4 SSCs under control condition (black) and in the presence of 10 µM of AppCH$_2$ppA (red). (*H*) Summary data of sEPSC frequencies. Data are presented as mean ± SEM, $^*P < 0.05$, $^{**}P < 0.001$ and $^{***}P < 0.001$. (*D*) $n = 10$ cells for control, AppCH$_2$ppA and washout, $n = 5$ cells for AppCH$_2$ppA + DPCPX and $n = 3$ cells for AppCH$_2$ppA + ADA. (*E*) and (*F*) $n = 12$ cells for control and AppCH$_2$ppA. (*H*) $n = 9$ cells for control and AppCH$_2$ppA, $n = 8$ cells for washout and $n = 5$ cells for AppCH$_2$ppA + DPCPX and AppCH$_2$ppA + ADA.

by AppCH$_2$ppA administration. Neither the amplitudes nor the durations of action potentials (APs) were changed significantly by AppCH$_2$ppA administration, suggesting that sodium channel activities were not being affected by the drug. AP initiation threshold potentials and AHP maximal amplitudes were also not significantly changed by AppCH$_2$ppA administration (−39.1 ± 0.7 mV under control conditions vs. −37.6 ± 0.9 mV in the presence of AppCH$_2$ppA, n = 23 cells, paired sample t-test, P = 0.21, Fig. 2A,B for AP threshold and 14.4 ± 0.6 mV under control conditions vs. 14.3 ± 0.9 mV in the presence of AppCH$_2$ppA, n = 9 cells, Wilcoxon test, P > 0.999, for AHP maximal amplitude). However, the input resistance derived from the slopes of I–V curves obtained in current clamp mode significantly decreased from 280.1 ± 0.02 MΩ in control condition to 225.9 ± 0.01 MΩ in the presence of 10 μM AppCH$_2$ppA (n = 9 cells, P = 0.016, Fig. 2A–C). The current rheobase was also significantly increased from 48.9 ± 6.6 pA under control condition to 75.6 ± 6.3 pA in the presence of AppCH$_2$ppA (n = 23 cells, Wilcoxon test, P = 0.0001) with a significant washout of this effect (56.2 ± 7 pA, n = 20 cells, Wilcoxon test, P = 0.002, Fig. 2A,B). The dependence of AP firing frequencies on injected current amplitudes (input–output curve) was shifted by AppCH$_2$ppA (Fig. 2D,E) with AP firing frequency at strong depolarizing currents being significantly decreased (15.89 ± 2.57 Hz under control condition, 8.22 ± 1.13 Hz in the presence of AppCH$_2$ppA, n = 9 cells, P = 0.01 with a 190 pA current amplitude, Fig. 2D–F). Altogether these data suggest that AppCH$_2$ppA reduces the excitability of SCCs.

AppCH$_2$ppA Induces Adenosine-Dependent Activation of Potassium Channels in *Tsc1*$^{+/-}$ Mice

A positive shift in a holding current following the application of AppCH$_2$ppA in whole-cell recordings (Fig. 1A) and a reduction of membrane resistance (Fig. 2B,C) imply activation of hyperpolarizing conductances that might be responsible for the overall reduction in excitability of layer 4 SSCs. To test this possibility, we performed cell-attached single channel recordings in the layer 4 SSCs in *Tsc1*$^{+/-}$ mice.

With Kglu pipette solution at a pipette potential of +30 mV, 82% of cells showed spontaneous single channel currents with a mean amplitude of 10.58 ± 0.44 pA that corresponds to an estimated single channel conductance of about 106 pS (n = 36 cells, Fig. 3A). Mean open and closed times were 1.02 ± 0.1 ms and 1275.7 ± 309.5 ms, respectively. Application of 10 μM AppCH$_2$ppA to the bath did not change the amplitude but dramatically altered the kinetics of these channels. The mean open time increased to 1.74 ± 0.2 ms, while the mean closed time decreased to 309.6 ± 111.4 ms and the opening frequency of the channels significantly increased from 4 ± 1.2 Hz under control conditions to 17.7 ± 3.9 Hz in the presence of AppCH$_2$ppA (n = 27; paired sample t-test, P = 0.002). Consequently, the open probability of the channels significantly increased (42.9 ± 15.3 of control, n = 27; paired sample t-test, P < 0.0001, Fig. 3B,C).

Activation of adenosine A1 receptors is known to induce tonic inhibition through potassium channels activation (Trussell and Jackson 1985; Sodickson and Bean 1998; Dunwiddie and Masino 2001; van Aerde et al. 2015). Indeed, bath application of 10 μM of adenosine increased open probability of potassium channels as expected, with a mean amplitude of 10.11 ± 0.73 pA and an estimated single-channel conductance of about 101 pS recorded in Kglu conditions (Fig. 3C), thereby pointing to the common mechanisms of adenosine and AppCH$_2$ppA actions. In cell-attached recordings in the presence of 40 nM of DPCPX or 10 μg/mL of ADA, application of 10 μM of AppCH$_2$ppA did not affect single channel activity (Fig. 3C) further confirming the involvement of adenosine and A1Rs in AppCH$_2$ppA effects on the activation of these channels. To confirm the K^+ dependency of single-channels activated by AppCH$_2$ppA we performed experiments with a K^+ channel blocker: cesium. While recording with the Kglu-containing pipette showed single channel activity sensitive to AppCH$_2$ppA application, the recordings with the CsCl-containing pipette (simultaneously attached to the same cell) did not show either single channel activity or sensitivity to AppCH$_2$ppA in any of the 10 cells tested (Fig. 4A,B). To clarify the type of potassium channels involved in tonic inhibition induced by AppCH$_2$ppA we performed experiments with Tertiapin-Q, a selective G-protein coupled inward rectifier potassium (GirK) channel inhibitor (Hibino et al. 2010). In the presence of Tertiapin-Q, the effects of AppCH$_2$ppA on firing frequency (0.41 ± 0.10 of control n = 5 cells, P = 0.0625, Wilcoxon test) and rheobase (1.86 ± 0.20 of control, n = 5 cells, P = 0.0135, Wilcoxon test) were essentially unchanged (Fig. 4C), suggesting no major contribution of GirK. Recently it has been shown that another potassium channel: TREK (or K2P2.1 or KCNK2 channels, that belongs to the 2-pore-domain potassium channel family) can be stimulated by Gαi-coupled neurotransmitter receptors, including adenosine (Lesage and Lazdunski 2000; Mathie et al. 2010; Rotermund et al. 2018). Consistent with this, the administration of bupivacaine, a selective blocker of TREK channels (Lesage and Lazdunski 2000; Punke et al. 2003; Shin et al. 2014), blocked the effects of AppCH$_2$ppA on firing frequency (0.93 ± 0.07 of control, n = 7 cells, P = 0.3559) and rheobase (1.08 ± 0.05 of control, n = 7 cells, P = 0.1444) in similar experiments (Fig. 4C). Moreover, the positive shift of holding current recorded in whole cell configuration in the presence of AppCH$_2$ppA (11.9 ± 1.4 pA, n = 13) was completely abolished in the presence of 500 μM of Bupivacaine (−0.31 ± 0.72 pA, n = 9) (Fig. 4D,E). Taken together, these data suggest that TREK channels are highly likely to be primary mediators of the effects of AppCH$_2$ppA.

In control ACSF, 10 out of 44 SSCs of *Tsc1*$^{+/-}$ mice, recorded in cell-attached mode with the pipettes containing Kglu solution showed spontaneous AP firing. Bath application of 10 μM AppCH$_2$ppA reversibly reduced the spiking frequency to 0.3 ± 0.1 of control (n = 10; Wilcoxon test, P = 0.006) in parallel with increased single channels activity (Fig. 5A,B,D). In 6 out of 10 cells we observed a complete block of AP firing, that was restored after AppCH$_2$ppA washout (Fig. 5A,B). These experiments directly indicated that AppCH$_2$ppA-mediated activation of potassium channels reduced excitability of SSCs. In similar recordings in the presence of DPCPX, or ADA, 10 μM of AppCH$_2$ppA did not affect spontaneous AP firing (Fig. 5D) further confirming that AppCH$_2$ppA effects are mediated by increased adenosine levels and subsequent activation of A1Rs.

AppCH$_2$ppA Mediates a Neuronal Release of Adenosine

To test whether these findings obtained in *Tsc1*$^{+/-}$ mice might be translated to human patients with TSC, we performed studies in human postsurgical tissue. Cell-attached recordings in brain slices from cortical neurons showed bursting spontaneous AP firing (Supplementary Fig. S2). Application of 10 μM AppCH$_2$ppA increased single channel activity that was followed by complete block of AP firing, that returned after AppCH$_2$ppA washout (Fig. 5C). As with *Tsc1*$^{+/-}$ mice, AppCH$_2$ppA administration significantly increased the single channel open probability (from 0.004 ± 0.002 to 0.22 ± 0.12, Wilcoxon test, P = 0.002), the opening frequency of the channels (from 7.4 ± 5.1 Hz

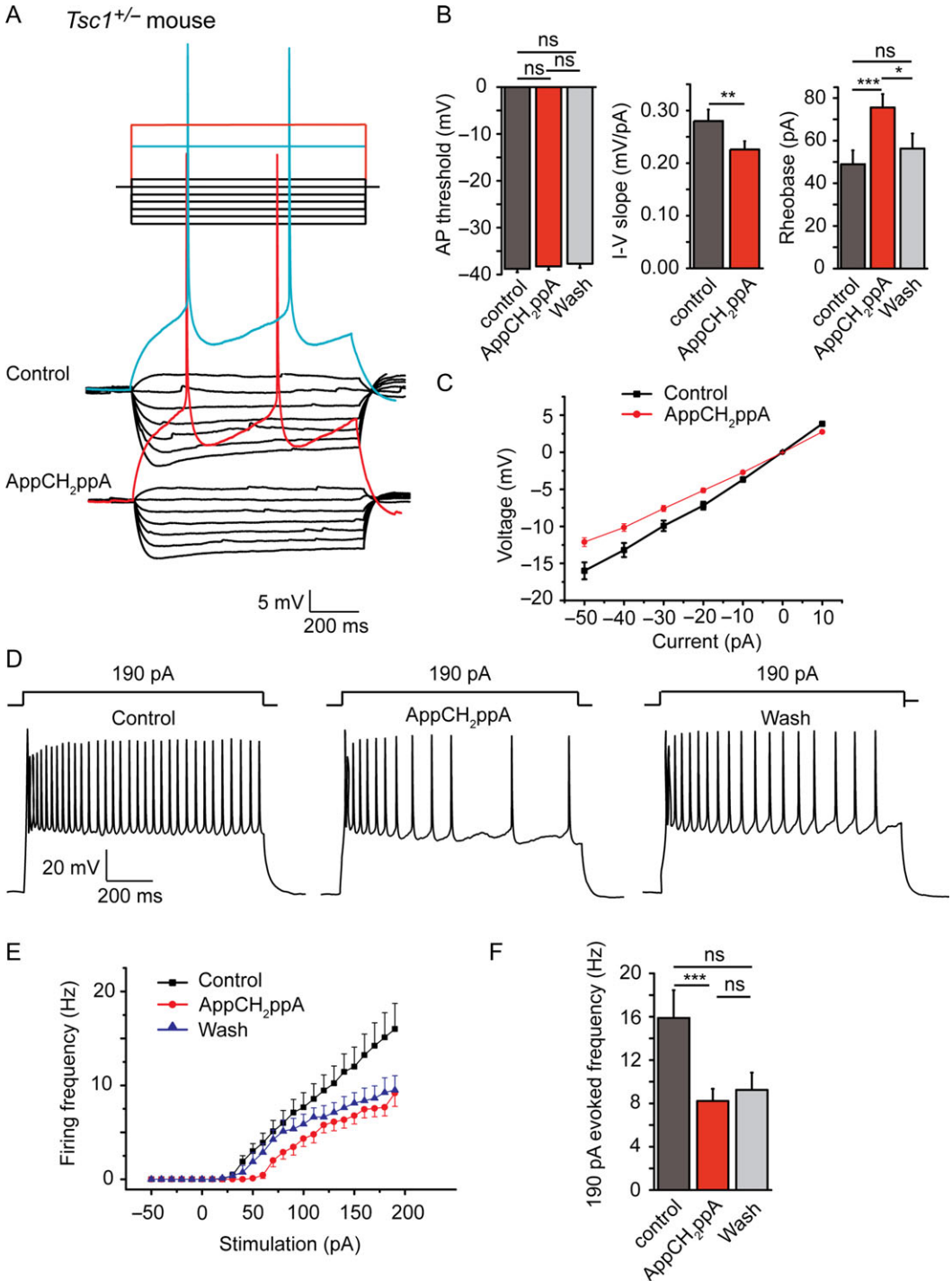

Figure 2. AppCH$_2$ppA reduces excitability of layer 4 SSCs. (*A*) Representative traces of membrane potentials recorded in layer 4 SSC in current clamp mode in *Tsc1*$^{+/-}$ mouse in response to the stepwise current injections (top) in control (middle) and with 10 μM AppCH$_2$ppA (bottom). Rheobase currents and corresponding responses are represented for control (blue) and AppCH$_2$ppA application (red). (*B*) Summary data for the AP firing threshold potentials (left), slopes of the current–voltage (*I–V*) curves shown on (*C*) (middle) and the rheobase (right). (*C*) *I–V* relations obtained by the protocol shown by black traces in ((*A*), top) in control and with 10 μM AppCH$_2$ppA. (*D*) Representative traces of membrane voltages recorded following 190 pA depolarizing current steps in control (left), with 10 μM AppCH$_2$ppA (middle) and after washout (right). (*E*) Dependence of the AP frequency on the amplitude of injected current (input–output curve). (*F*) Summary data for AP frequency induced by 190 pA depolarizing current steps. Data are presented as mean ± SEM, *$P < 0.05$, **$P < 0.001$ and ***$P < 0.001$. (*B*) $n = 9$ cells for control, AppCH$_2$ppA and washout. (*F*) $n = 9$ cells for control and AppCH$_2$ppA and $n = 8$ cells for washout.

to 73.6 ± 38.3 Hz, Wilcoxon test, $P = 0.002$) and decreased the channels mean closed time (from 34 852 ± 17556 ms to 55.1 ± 22.3 ms, Wilcoxon test, $P = 0.002$, Fig. 5E).

This suggests that as in *Tsc1*$^{+/-}$ mice, AppCH$_2$ppA may suppress epilepsy associated with TSC in human patients through strong activation of potassium channels.

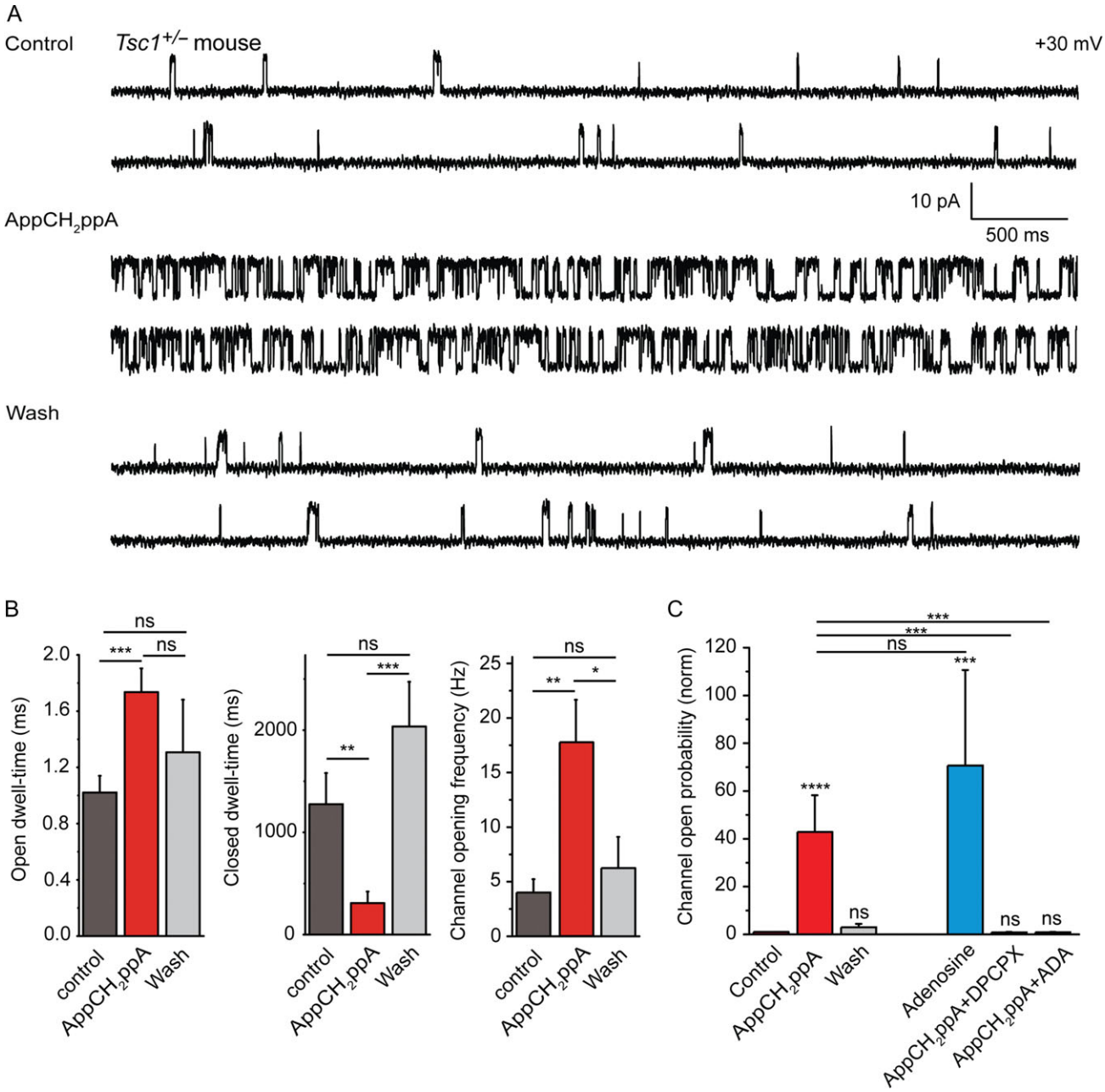

Figure 3. $AppCH_2ppA$ activates single channels in SSCs in adenosine- and A1R-dependent manner. (*A*) Representative traces of spontaneous single channels activity of layer 4 SSCs in $Tsc1^{+/-}$ mouse slice recorded in cell-attached mode at the pipette potential of +30 mV. Note dramatic increase in channels activity following $AppCH_2ppA$ application. (*B*) Summary data for the $AppCH_2ppA$ effects on channels mean open times, mean closed times and opening frequencies. (*C*) Summary data for the effects on channel open probabilities of 10 μM $AppCH_2ppA$, 10 μM adenosine and 10 μM $AppCH_2ppA$ in the presence of 40 nM DPCPX or 10 μg/mL ADA. Data are presented as mean ± SEM, $^*P < 0.05$, $^{**}P < 0.001$ and $^{***}P < 0.001$. (*B*) $n = 27$ cells for control and $AppCH_2ppA$ and $n = 22$ cells for washout. (*C*) $n = 27$ cells for control and $AppCH_2ppA$, $n = 22$ cells for washout, $n = 11$ cells for adenosine, $n = 6$ cells for $AppCH_2ppA$ + DPCPX and $n = 5$ cells for $AppCH_2ppA$ + ADA.

$AppCH_2ppA$ Enhances Adenosine Signaling

To clarify the mechanisms of $AppCH_2ppA$-induced adenosine increase we performed experiments with the ecto-5′-nucleotidase (e5′NT) inhibitor: α,β-methylene-ADP. We found that the effects of $AppCH_2ppA$ were preserved in the presence of α,β-methylene-ADP. In particular, as with $AppCH_2ppA$ alone, administration of $AppCH_2ppA$ in the presence of α,β-methylene-ADP decreased the firing frequency to 0.65 ± 0.0033 of control (vs. 0.63 ± 0.085 of control by $AppCH_2ppA$ alone, $n = 10$ cells, $P = 0.8304$, Fig. 6*A*). Similarly effects of $AppCH_2ppA$ on rheobase were not affected in the presence of α,β-methylene-ADP (1.63 ± 0.14 of control vs. 1.65 ± 0.14 of control by $AppCH_2ppA$ alone, $n = 10$ cells, $P = 0.9375$, Fig. 6*B*). These data allow us to exclude the possibility that extracellular catabolism of ATP is the source of adenosine. Instead, adenosine might be generated intracellularly by $AppCH_2ppA$-mediated inhibition of ADK (Delaney et al. 1997)

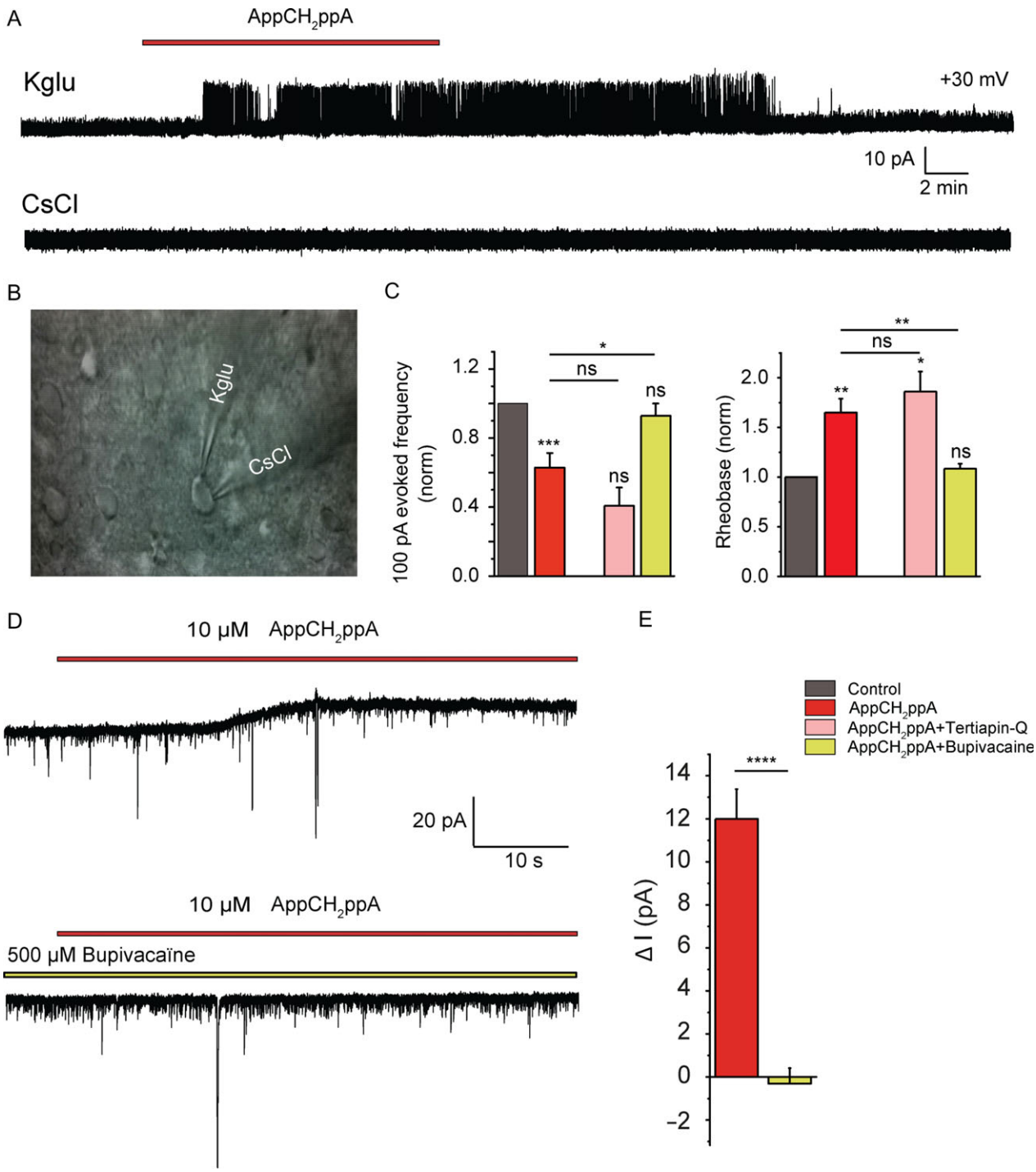

Figure 4. AppCH$_2$ppA activates specific potassium channels in SSCs. (*A*) Representative traces of spontaneous single channels activity of layer 4 SSCs in a *Tsc1*$^{+/-}$ mouse slice recorded in cell-attached mode at the pipette potential of +30 mV in control and in the presence of 10 µM of AppCH$_2$ppA with Kglu (top) and CsCl (bottom) pipette solutions. (*B*) DIC image of SSC in a *Tsc1*$^{+/-}$ mouse slice patched simultaneously with 2 pipettes filled with the 2 different solutions. (*C*) Summary data for normalized rheobases and AP frequencies induced by 100 pA depolarizing current steps in control condition, with 10 µM AppCH$_2$ppA and with 10 µM AppCH$_2$ppA in the presence of 100 nM Tertiapin-Q or 500 µM Bupivacaine. (*D*) Representative traces of the holding current recorded in voltage clamp whole-cell at −70 mV after application of 10 µM AppCH$_2$ppA (top) and 10 µM AppCH$_2$ppA in the presence of 500 µM of Bupivacaine (bottom). (*E*) Summary data for the holding current amplitude shifts for both conditions. The color coding shown is applied to panels (*C*) and (*E*). Data are presented as mean ± SEM, *$P < 0.05$, **$P < 0.001$ and ****$P < 0.0001$. (*C*) $n = 15$ cells for control and AppCH$_2$ppA, $n = 5$ cells for AppCH$_2$ppA + Tertiapin-Q and $n = 7$ cells for AppCH$_2$ppA + Bupivacaine. (*E*) $n = 13$ cells for AppCH$_2$ppA and $n = 9$ cells for AppCH$_2$ppA + Bupivacaine.

and released through the equilibrative nucleoside transporters (ENT) ENT1 and ENT2 (Brundege and Dunwiddie 1998; Lovatt et al. 2012).

To find out whether or not adenosine is released from neurons, we used inosine as a competitive inhibitor of adenosine efflux (Ward et al. 2000; Lovatt et al. 2012) from the cell

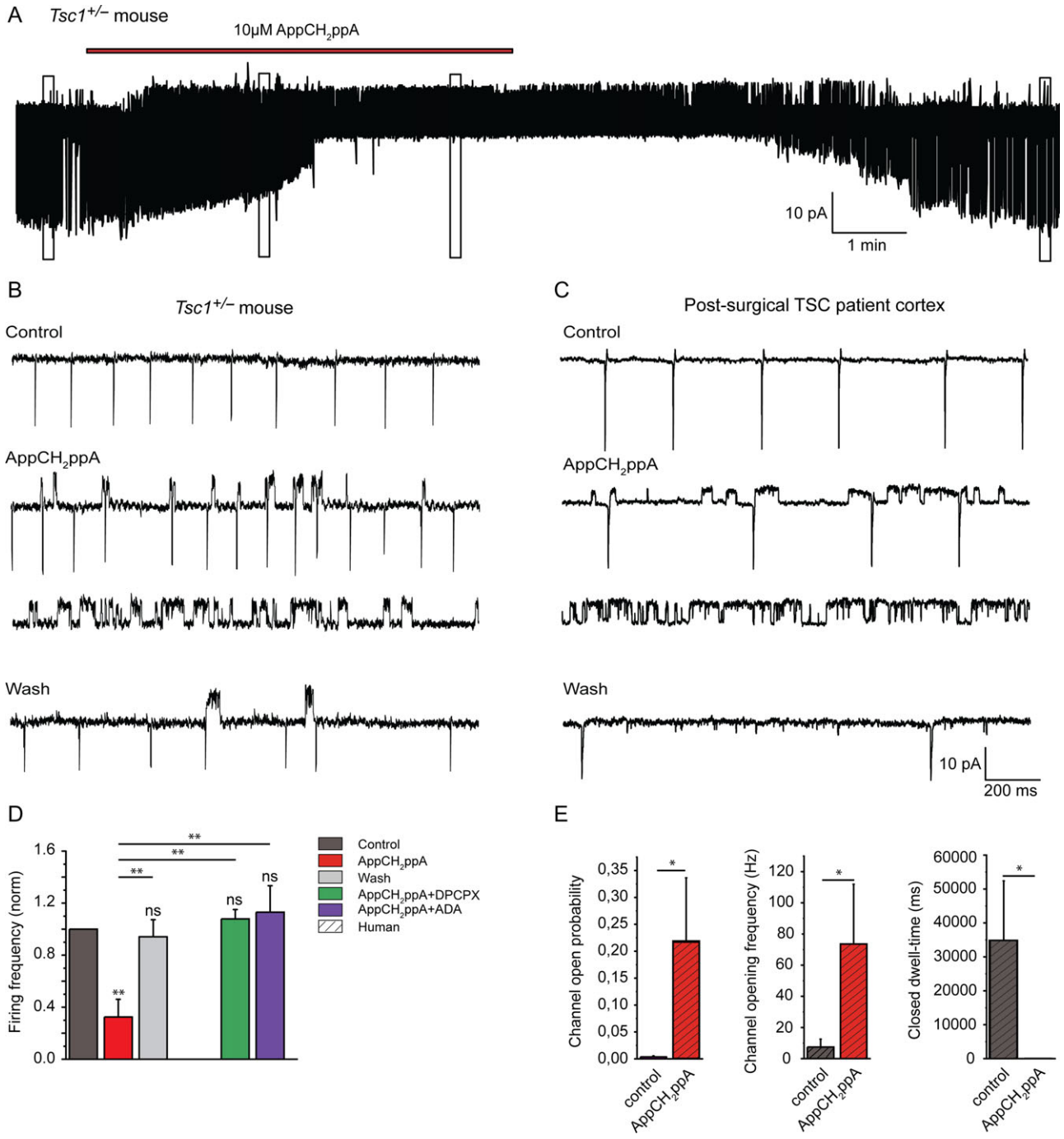

Figure 5. $AppCH_2ppA$ reduces neuronal spontaneous spiking by activating potassium channels in $Tsc1^{+/-}$ mice and in human postoperational tissue. (*A*) Representative trace of the spontaneous activity of layer 4 SSCs in a $Tsc1^{+/-}$ mouse slice recorded in cell-attached mode at the pipette potential of +30 mV in control condition, in the presence of 10 μM of $AppCH_2ppA$ and after washout. (*B*) Extended traces (marked by boxes in (*A*)) showing channels activity in control condition, during wash-in of 10 μM of $AppCH_2ppA$, in the presence of $AppCH_2ppA$ and after washout, respectively (from top to bottom). (*C*) The same as in (*B*), but for the cell from a human brain postoperational slice from a TSC patient. (*D*) Summary data for the $AppCH_2ppA$ effects on normalized firing frequencies in cell-attached mode in control condition, with 10 μM $AppCH_2ppA$ and with 10 μM $AppCH_2ppA$ in the presence of 40 nM DPCPX or 10 μg/mL ADA. (*E*) Summary data for the $AppCH_2ppA$ effects on channel open probabilities, opening frequencies and mean closed times for the channels recorded in cell-attached mode from neurons in human brain postoperational slices of 2 TSC patients. Data are presented as mean ± SEM, $^*P < 0.05$ and $^{**}P < 0.001$. (*D*) $n = 10$ cells for control, $AppCH_2ppA$ and washout, $n = 5$ cells for $AppCH_2ppA$ + DPCPX and $AppCH_2ppA$ + ADA. (*E*) $n = 7$ cells for control and $AppCH_2ppA$ from 2 different TSC patients.

through the ENT. $AppCH_2ppA$ effects on neuronal excitability were completely blocked when inosine was added to the patch pipette solution (0.99 ± 0.02 of control evoked firing frequency and 0.98 ± 0.06 of control rheobase, $n = 9$ cells, Wilcoxon test, Fig. 6A,B). Interestingly the effects of $AppCH_2ppA$ were completely preserved in a neighboring neuron, located in close proximity to the inosine loaded neuron, when excitability was recorded simultaneously using a patch pipette containing control intracellular solution (Fig. 6).

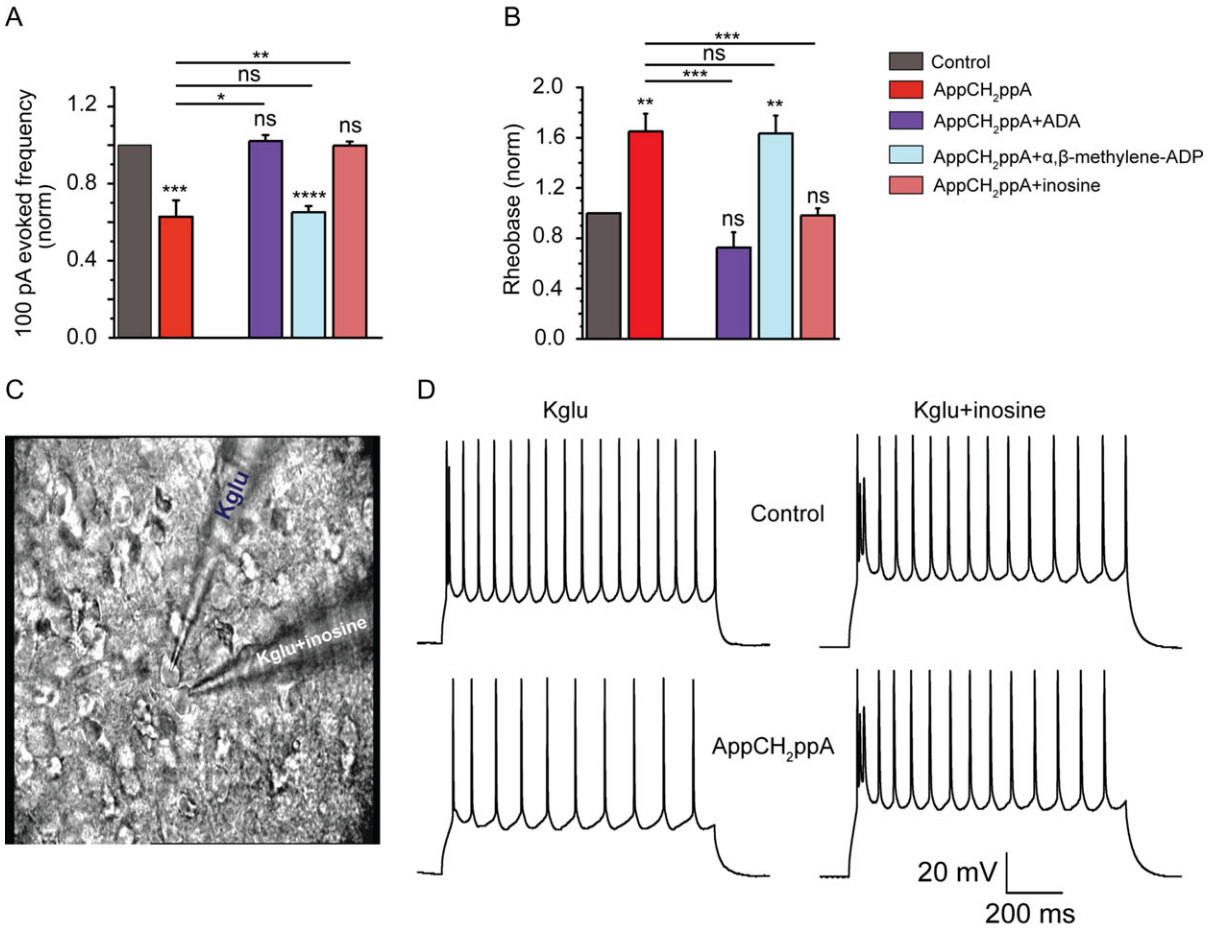

Figure 6. AppCH$_2$ppA induces direct release of adenosine from recorded neurons. (*A*) Summary data for normalized AP frequencies induced by 100 pA depolarizing current steps in control condition, with 10 μM AppCH$_2$ppA and with 10 μM AppCH$_2$ppA in the presence of 10 μg/mL ADA, 100 μM α,β-methylene-ADP or 100 μM inosine. (*B*) Summary data for normalized rheobases in control condition, with 10 μM AppCH$_2$ppA and with 10 μM AppCH$_2$ppA in the presence of 10 μg/mL ADA, 100 μM α,β-methylene-ADP or 100 μM inosine. (*C*) DIC image of 2 SSCs in a *Tsc1*$^{+/-}$ mouse slice patched simultaneously one with a pipette containing Kglu solution the other with a pipette containing Kglu + 100 μM inosine. (*D*) Representative traces of membrane voltages following 100 pA depolarizing current steps in control (top) and in the presence of 10 μM of AppCH$_2$ppA (bottom). Whole-cell recordings were made from the cells shown in (*C*), one loaded with a standard Kglu solution (left) and the other with solution containing Kglu +100 μM inosine (right). Data are presented as mean ± SEM, *$P < 0.05$, **$P < 0.001$ and ***$P < 0.001$. (*A*) and (*B*) $n = 15$ cells for control and AppCH$_2$ppA, $n = 6$ cells for AppCH$_2$ppA + ADA, $n = 10$ cells for AppCH$_2$ppA + α,β-methylene-ADP and $n = 9$ cells for AppCH$_2$ppA + inosine.

These results suggest that adenosine is directly released from single neurons by AppCH$_2$ppA in a strictly localized manner. The exact mechanism of AppCH$_2$ppA-induced adenosine release remains unknown. However, nonselective P2X/P2Y antagonist: suramin, but not selective P2Y1 antagonist: MRS2500, completely prevented the effects of AppCH$_2$ppA, indicating the contribution of P2X/P2Y receptors in the AppCH$_2$ppA mediated effects (Supplementary Fig. S3).

AppCH$_2$ppA Decreases Temporal Summation of Synaptic Input Through Postsynaptic Mechanism

Given the foregoing data, AppCH$_2$ppA administration appears to induce antiepileptic effects through strictly localized adenosine release from single neurons. To investigate whether AppCH$_2$ppA may also affect presynaptic A1Rs we analyzed changes to the integrative properties of layer 4 SSCs following AppCH$_2$ppA administration. For this we recorded evoked EPSPs (eEPSPs) in SSCs triggered by extracellular stimulation of cortical layer 4 horizontal recurrent connections (see Materials and Methods). The bath application of 10 μM of AppCH$_2$ppA significantly and reversibly decreased eEPSPs amplitude to 0.68 ± 0.06 of control ($n = 6$, Wilcoxon test $P = 0.0035$) and decay kinetics, determined by the charge transfer of the eEPSPs normalized by amplitudes, to 0.73 ± 0.03 of control ($n = 6$, Wilcoxon test, $P = 0.0002$, Fig. 7A,C). Consequently, the absolute charge transfer of the evoked depolarization significantly decreased to 0.56 ± 0.06 in the presence of AppCH$_2$ppA compared with control ($n = 6$, 0.87 ± 0.18 after washout; Wilcoxon test, $P = 0.03$).

This suggests that AppCH$_2$ppA might reduce temporal summation window during repetitive high-frequency stimulation. To test this, we applied a train of 5 consecutive stimulations at 50 Hz. Under control conditions, train stimulation evoked typical plateau shaped eEPSPs (train eEPSPs). In the presence of 10 μM AppCH$_2$ppA, the plateau was abolished and the normalized charge transfer decreased to 0.43 ± 0.09 of control ($n = 5$, Wilcoxon test, $P = 0.003$, Fig. 7B,D). The effect of AppCH$_2$ppA on normalized charge transfer in train eEPSPs (0.43 ± 0.09) was significantly larger than found with single eEPSPs (0.73 ± 0.03) ($P = 0.03$).

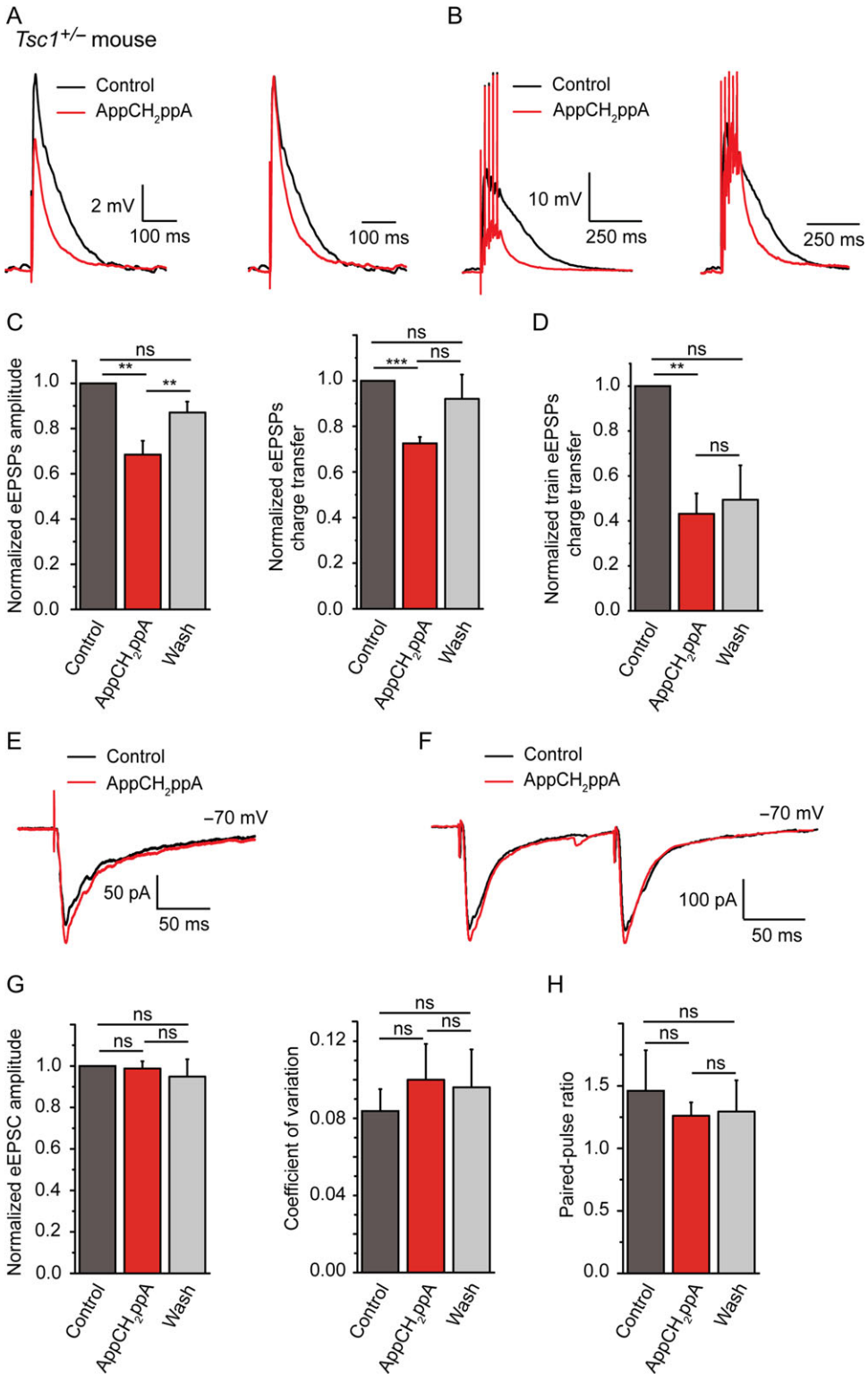

Figure 7. AppCH$_2$ppA reduces the temporal summation window of inputs to layer 4 SSCs by a postsynaptic mechanism. (*A*) Absolute (left) and normalized (right) representative traces of EPSPs evoked by single stimulation in layer 4 SSCs in a *Tsc1*$^{+/-}$ mouse slice (eEPSPs) recorded in current clamp. (*B*) Absolute (left) and normalized (right) representative traces of EPSPs evoked by a train of 5 stimuli (at 50 Hz) in layer 4 SSCs in a *Tsc1*$^{+/-}$ mouse slice (train eEPSPs) recorded in current clamp. (*C*) Summary data for the AppCH$_2$ppA effects on mean eEPSP amplitudes (left), and mean normalized by peak charge transfer (right) relative to control. (*D*) Summary data for the AppCH$_2$ppA effects on train eEPSPs charge transfers normalized by last peak relative to control. (*E*) Representative traces of evoked eEPSCs in layer 4 SSCs in *Tsc1*$^{+/-}$ mouse slice recorded in voltage clamp at −70 mV. (*F*) Representative traces of eEPSCs evoked by paired-pulse stimulation in layer 4 SSCs in a *Tsc1*$^{+/-}$ mouse slice recorded in voltage clamp at −70 mV. (*G*) Summary data for the AppCH$_2$ppA effects on eEPSC mean amplitudes and coefficients of variation. (*H*) Summary data for paired-pulse ratios of eEPSCs. Data are presented as mean ± SEM, $^{**}P < 0.001$ and $^{***}P < 0.001$. (*C*) $n = 6$ cells for control and AppCH$_2$ppA and $n = 3$ cells for washout. (*D*) $n = 5$ cells for control, AppCH$_2$ppA and washout. (*G*) $n = 6$ cells for control, AppCH$_2$ppA and washout. (*H*) $n = 5$ cells for control, AppCH$_2$ppA and washout.

eEPSCs in layer 4 SSCs of *Tsc1*$^{+/-}$ mouse slice triggered by single extracellular stimulation of cortical layer 4 were notably not altered by AppCH$_2$ppA. Application of 10 μM AppCH$_2$ppA changed neither eEPSCs amplitude (0.98 ± 0.03 of control in the presence of AppCH$_2$ppA; Wilcoxon test, $P = 0.999$), nor the coefficient variation of eEPSC amplitudes (0.08 ± 0.01 in control and 0.10 ± 0.02 in the presence of AppCH$_2$ppA; paired sample t-test, $P = 0.2$) (Fig. 7*E*,*G*), nor paired-pulse ratios (PPRs) of eEPSCs (PPR was 1.46 ± 0.32 in control and 1.26 ± 0.11 in the presence of AppCH$_2$ppA; Wilcoxon test, $P = 0.999$) (Fig. 7*F*,*H*). This indicates that AMPAR-mediated synaptic transmission remains intact in the presence of AppCH$_2$ppA. This is in contrast to the effects of adenosine, since bath application of 10 μM of adenosine significantly reduced eEPSC amplitudes (Supplementary Fig. S4A, B) indicative of local restrictions to AppCH$_2$ppA inhibitory mechanisms compared with those of bath applied adenosine.

Taken together, these data suggest that AppCH$_2$ppA produced strong antiepileptic effect by significantly reducing the temporal summation window of recurrent excitation in layer 4 SSCs, thus, preventing seizure generation without affecting synaptic release.

AppCH$_2$ppA Reduces Discharges in In Vitro Pharmacological Model of Epilepsy

The general mode of action of AppCH$_2$ppA (mainly reducing neuronal excitability revealed in TSC) implies that this compound may have antiepileptic effects in other types of epilepsies. Therefore, we tested the effects of AppCH$_2$ppA in a robust pharmacological model of epilepsy induced by lowering Mg^{2+} and blocking inhibition by $GABA_AR$ antagonist (Avoli et al. 2002; Reddy and Kuruba 2013). For this, we performed whole-cell current clamp recordings from hippocampal CA1 pyramidal neurons in wild type mouse brain slices in Mg^{2+}-free, picrotoxin (100 μM) containing extracellular solution. Under these conditions neurons displayed spontaneous, repetitive, high-frequency action potential firing exhibiting seizure-like epileptiform activity consisting of bursting events of 3–7 s duration. (Supplementary Fig. S5A). Bath application of AppCH$_2$ppA reversibly reduced the frequency of this epileptic bursts in a concentration-dependent manner (Supplementary Fig. S5A, B). Thus, AppCH$_2$ppA exerts an antiepileptic effect also in general in vitro pharmacological model of epilepsy.

AppCH$_2$ppA Reduces Spontaneous Epileptic Crisis In Vivo in *Tsc1*$^{+/-}$ Mice

Finally, we tested the antiepileptic actions of AppCH$_2$ppA in vivo by performing intracortical electroencephalography (EEG) recordings in somatosensory S1 cortex of head restrained, nonanaesthetized, *Tsc1*$^{+/-}$ mice at postnatal days P14–P16. Spontaneous recurrent seizures spreading in all layers of somatosensory cortex recorded in control conditions were strongly depressed by intraperitoneal (i.p.) injections of AppCH$_2$ppA at a dose of 83 mg/kg of animal body weight (Fig. 8). By contrast *Tsc1*$^{+/-}$ mice i.p. injected with vehicle or in control noninjected *Tsc1*$^{+/-}$ mice, the recurrent epileptic discharges persisted up to several hours (Fig. 8*E*). We conclude that this nonhydrolysable analogue of the diadenosine-tetraphosphate family has powerful in vivo antiepileptic action in *Tsc1*$^{+/-}$ mice.

Some of the major expected side effects from central adenosine receptors activation are hypothermia (Tupone et al. 2013) or heart dysfunction (Mustafa et al. 2009; Li et al. 2016). To test whether AppCH$_2$ppA may produce similar effects, we measured the body weight and temperature of the *Tsc1*$^{+/-}$ mice within 2 days following the injection of AppCH$_2$ppA. These values were not significantly different from those measured in noninjected mice kept under the same conditions (Supplementary Fig. S6A, B, Supplementary Table S2). Mice heartbeat rates measured during the EEG recordings (see Methods) also did not show any significant differences following the AppCH$_2$ppA i.p. injection (317.9 ± 23.1 beats/min before, and 320.5 ± 20.7 beats/min after AppCH$_2$ppA i.p. injection, $n = 5$, $P = 0.521$, Supplementary Fig. S6C, D).

Altogether, these results indicate that AppCH$_2$ppA at the concentration used to eliminate seizures does not disturb the main vital autonomous functions of the treated mice, consistent with a localized mechanism of action of the compound.

Discussion

We have previously shown that the *Tsc1*$^{+/-}$ mouse model exhibits an increased temporal summation of excitatory inputs in layer 4 SSCs providing a source of network hypersynchronization and self-generated long-lasting epileptic activity (Lozovaya et al. 2014).

The data reported here suggest that in layer 4 SSCs, AppCH$_2$ppA stimulates local neuronal adenosine release that, by a postsynaptic A1R-dependent mechanism, activates potassium channels resulting in a reduction of SSCs excitability. This limits the temporal summation of excitatory inputs and network hypersynchronicity leading to disruption of the excitation loop necessary to generate epileptic waves. Consequently, AppCH$_2$ppA exerts strong antiepileptic action in the *Tsc1*$^{+/-}$ mouse model in vitro and in vivo as well as in the resected brain tissues of TSC patients. By reducing neuronal excitability, AppCH$_2$ppA is also a good candidate to block other types of epilepsies, as illustrated by its efficient blocking of crisis in a more general in vitro pharmacological model of epilepsy.

Our data clearly demonstrate that effects of AppCH$_2$ppA are mediated by an increase of adenosine levels rather than by a direct interaction with A1Rs. Otherwise bath ADA application or the loading of neurons with intracellular inosine would not have prevented the effects of AppCH$_2$ppA as observed. In addition, since AppCH$_2$ppA was applied directly in the bath, if direct A1R activation was taking place, then AppCH$_2$ppA would also activate presynaptic as well as postsynaptic A1Rs, which was not observed to be the case.

In keeping with extensive data in different epileptic models, a low adenosine levels is a risk factor for the emergence of epilepsy (Glass et al. 1996; Dunwiddie and Masino 2001; Rebola et al. 2003; Boison 2005, 2012), hence, the enhancement of adenosine signaling by AppCH$_2$ppA appears a biologically powerful means to control epileptiform activity. Although adenosine can increase seizure threshold via A1Rs, it can also enhance seizure susceptibility via A2ARs (El Yacoubi et al. 2008, 2009). However, in our study we did not observe any proconvulsive effects of AppCH$_2$ppA—for example, in vivo EEG recordings did not show any exacerbation of seizures following the injection of compound. In contrast to inhibitory action of A1Rs, A2ARs activation is associated with a facilitation of excitatory transmission (viz., an increase in glutamate release) (Cunha 2001). However, we did not detect any rebound facilitatory effects after AppCH$_2$ppA washout in in vitro experiments (although this is typically observed with adenosine). Furthermore, the antagonist DPCPX, used at a concentration selective for A1Rs, completely blocked the inhibitory effects of

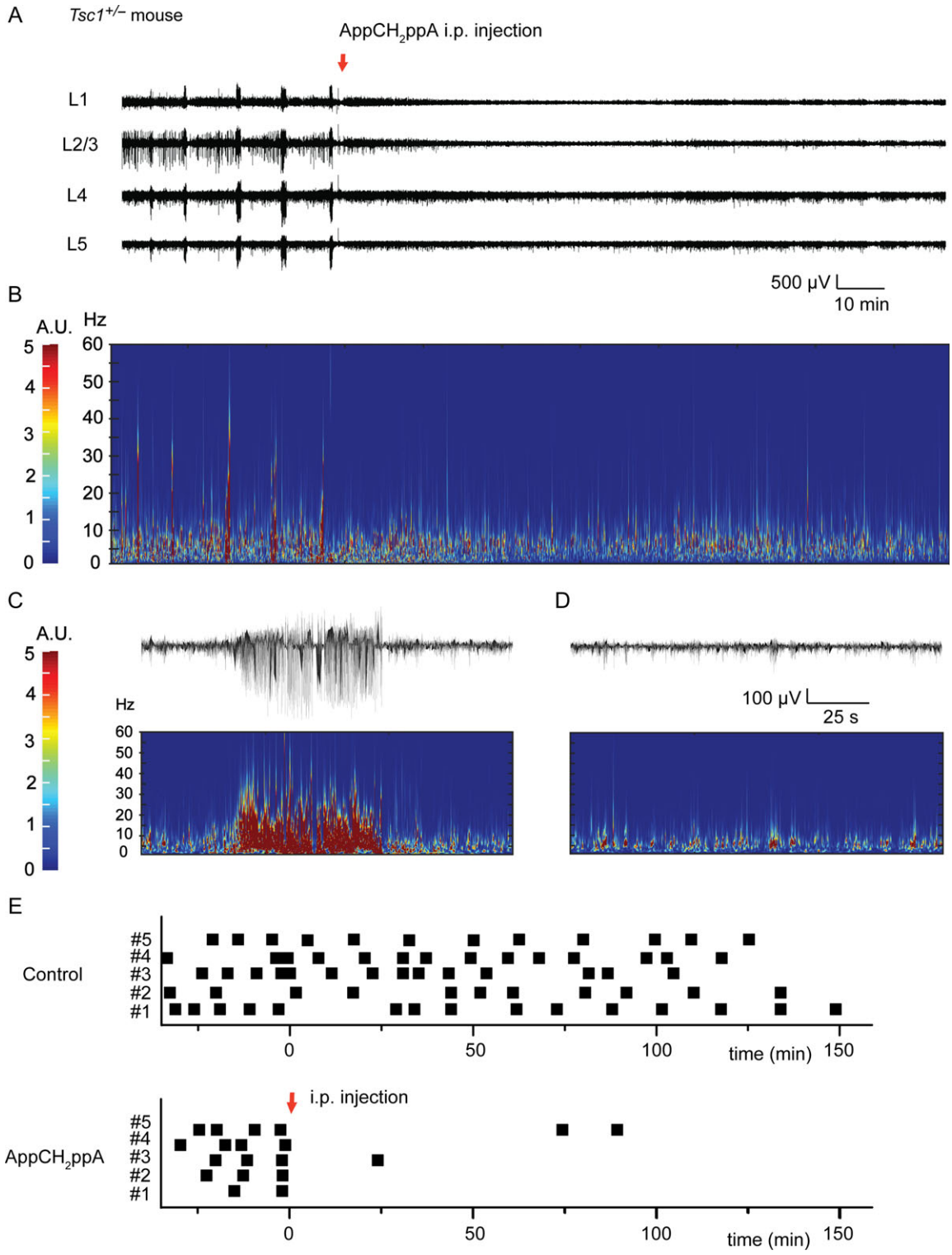

Figure 8. Acute antiepileptic effect of i.p. administration of AppCH$_2$ppA in vivo. (*A*) Intracortical EEG recordings in head-restrained P15 *Tsc1*$^{+/-}$ mouse before and after i.p. administration of AppCH$_2$ppA indicated by arrow. The upper trace corresponds to the superficial intracortical electrode placed at 100 µm from the pia. (*B*) Representation of wavelet spectrogram of the EEG trace corresponding to the layer 4 shown in (*A*). (*C*) Extended trace of an epileptiform crisis (top) with its related wavelet spectrogram (bottom). (*D*) Extended crisis-free trace after AppCH$_2$ppA injection (top) with its related wavelet spectrogram (bottom). (*E*) Time course of spontaneous seizure activity in *Tsc1*$^{+/-}$ mice at P14–P16 without (top) and with i.p. administration of AppCH$_2$ppA indicated by arrow. Individual seizures are represented by black squares. Each row (#) represents an individual experiment. A.U., arbitrary unit.

AppCH$_2$ppA and did not reveal any facilitatory effects of A2ARs, which could have been masked by A1Rs-mediated strong inhibitory effects. In addition, in the presence of ADA (which allows for the contribution of others adenosine receptors to be ruled out) the effects of AppCH$_2$ppA were seen not significantly different from those effects seen with DPCPX.

Hence, any involvement of A2ARs in mediating the effects of AppCH$_2$ppA is negligible.

In line with this notion, evidence obtained in previous studies using immunochemical methods and binding of A2AR ligands in synaptosomes suggested that there were much lower A2AR levels in the cerebral cortex than in other brain regions (e.g., in striatum) (Cunha et al. 1996; Lopes et al. 1999, 2004; Marchi et al. 2002). Therefore, because A1Rs have higher affinity to adenosine and because their expression in the cortex is much higher than of the other adenosine receptor subtypes (Fredholm et al. 2001; Ciruela 2011), the effects of AppCH$_2$ppA at concentrations used should be dominated by A1Rs contribution. However, the possible modulation of A1Rs activity by A2ARs in observed phenomena cannot be entirely excluded (Lopes et al. 1999).

The activation of cortical A1Rs by adenosine or agonists is known to suppress synaptic transmission through pre- or both pre- and postsynaptic mechanisms depending on cell type and cortical layer (Mathew et al. 2008; van Aerde et al. 2015; Zhang et al. 2015). The activation of postsynaptic A1Rs increases K^+ influx via different potassium channels, leading to membrane hyperpolarization and subsequent inhibition (Siggins and Schubert 1981; Yamada et al. 1998; Takigawa and Alzheimer 1999; Haas and Selbach 2000).

Postsynaptic A1R-dependent potassium channels activation has been shown to be responsible for the shunting of postsynaptic currents and increasing the rheobase (Dunwiddie and Masino 2001). In alignment with this, AppCH$_2$ppA application led to the appearance of an outward shift in the holding current in accordance with K^+ channels activation. Cell-attached recordings confirmed the enhancement of K^+ channels activity by AppCH$_2$ppA and the reduction of spontaneous spikes both in *Tsc1*$^{+/-}$ mice and in resected tissues from human TSC patients. The *I*–*V* curve analysis revealed that AppCH$_2$ppA decreased neuronal input resistance, confirming the activation of membrane conductances that are mostly responsible for the rheobase increase. In keeping with this, the amplitudes of eEPSPs were reduced and their kinetics were accelerated. The accelerated eEPSPs repolarization observed in the presence of AppCH$_2$ppA might account for the decrease of burst appearance induced by AppCH$_2$ppA, by the reduction of inputs temporal summation.

In our experiments the use of Tertiapin-Q did not affect AppCH$_2$ppA inhibitory effects, thereby excluding any major contribution of GirKs. By contrast, a TREK channel blocker completely abolished tonic inhibition induced by AppCH$_2$ppA. In our experiments roughly estimated single-channel conductance of AppCH$_2$ppA (106 pS) and adenosine-activated potassium channels (101 pS) and their kinetic parameters are comparable with those reported for TREK channels, 100 pS (Lesage and Lazdunski 2000). Thus, it is highly likely that AppCH$_2$ppA induces its effects in SSCs by activating TREK channels through adenosine.

Kruglikov and Rudy (2008) showed that, in addition to the activation of potassium channels, adenosine inhibits synaptic transmission in cortical networks by reducing presynaptic release. In our experiments bath application of adenosine also reduced eEPSC amplitudes most likely reducing presynaptic release probability via presynaptic A1Rs. However, it did not affect eEPSCs amplitude, CV, or PPR. These observations suggest that (in contrast to the bulk adenosine effects) AppCH$_2$ppA acts via a selective postsynaptic A1Rs-dependent mechanism without affecting presynaptic sites.

Several lines of evidence obtained in the present study indicate that AppCH$_2$ppA induces neuronal release of adenosine in a strictly localized manner, leading to A1Rs-dependent postsynaptic tonic inhibition. Firstly, our experiments with the extracellular application of ADA confirmed that AppCH$_2$ppA effects are mediated by adenosine.

Secondly, the inability of e5′NT inhibitor to prevent the effects of AppCH$_2$ppA excludes the possibility that these effects are mediated by adenosine coming from catabolism of extracellular ATP (Dunwiddie et al. 1997; Cunha et al. 1998), released from astrocytes (Rodrigues et al. 2015), microglia (Koizumi et al. 2013), endothelial cells or neurons (Fields 2011).

Thirdly, experiments with loading a single neuron with inosine indicate that AppCH$_2$ppA induces neuronal release of adenosine. Delaney et al. (1997) have shown that in brain homogenate AppCH$_2$ppA inhibits ADK with IC_{50} 1.9 μM, which is in the range of concentration we used in current studies. Thus, adenosine could be accumulated intracellularly as a result of ADK inhibition and released directly through the transporters ENT1 and ENT2 (Brundege and Dunwiddie 1998; Wall et al. 2007; Wall and Dale 2008). At this stage, the hypothesis on the ADK involvement is limited by the observation that ADK expression is shifted from neurons to astrocytes during development, being mainly present in astrocytes in adult mice (Studer et al. 2006). However, our investigation tackles an intermediate developmental age (P13–15) where a residual neuronal ADK expression cannot be excluded and could participate to the regulation of intracellular adenosine level.

Elevation of extracellular adenosine by traditional ENT blockers was interpreted as a result of inhibition of adenosine uptake into surrounding cells (including astrocytes, neurons) rather than direct adenosine release, which dominates the effects of ENT inhibition on extracellular nucleoside in a simulation study (Newby 1986; Yamashiro and Morita 2017). The bulk increase of extracellular adenosine (produced, e.g., by extracellular application of dipyridamole) would saturate A1R-related pathways and prevent AppCH$_2$ppA effects. Therefore, we elected to use intracellular inosine as a competitive inhibitor of adenosine efflux (Ward et al. 2000; Lovatt et al. 2012). Loading a single neuron with inosine completely blocked AppCH$_2$ppA effects in this cell. Whereas in the neurons loaded with the control intracellular solution, even in those located in a close proximity to the inosine loaded cell, the effects of AppCH$_2$ppA were preserved. The latter indicates that AppCH$_2$ppA triggers a spatially restricted release of adenosine from neurons.

Recent investigation has shown that effects of hyperexcitability-mediated release of adenosine are locally restricted due to active removal mechanisms (Wall and Richardson 2015) that limit diffusion. Together with our data from inosine, the absence of presynaptic effects of AppCH$_2$ppA can be explained therefore by a highly spatially restricted release of adenosine selectively from single neurons through ENT1 or 2, activating only local postsynaptic A1Rs of the same neuron, without affecting the presynaptic site due to active adenosine removal. Interestingly it has been found that ENT1 and A1Rs are highly colocalized (Jennings et al. 2001). Therefore, AppCH$_2$ppA can be considered as a regulator of local endogenous adenosine level that can influence locally the efficiency of adenosine signaling.

In spite of this, the exact mechanisms of AppCH$_2$ppA-induced adenosine release still remain to be elucidated fully. The fact that nonselective P2X/P2Y antagonist, suramin, completely prevented the effects of AppCH$_2$ppA, shown in our study, implies involvement of P2 receptors in these mechanisms. Thus, one may suggest that AppCH$_2$ppA might induce P2-dependent elevation of intracellular adenosine in neurons followed by its local release through the transporters ENT1 and

ENT2 (Brundege and Dunwiddie 1998; Brambilla et al. 2005; Lovatt et al. 2012).

Altogether, these considerations could explain the specific postsynaptic mechanisms of AppCH$_2$ppA antiepileptic action and the absence of the expected adenosine induced side effects in vivo. At the same time the scenario presented here does not specifically exclude the involvement of some alternative or additional mechanisms such as modulation of dinucleotide receptors by activation of adenosine receptors, as has been demonstrated in the rat hippocampal synaptosomes (Diaz-Hernandez et al. 2002). Such a modulation, as demonstrated for diadenosine polyphosphate and adenosine receptors, could reinforce effects of AppCH$_2$ppA.

In summary, in this study we have demonstrated the strong A1Rs-dependent adenosine antiepileptic effects of AppCH$_2$ppA. In contrast to adenosine, AppCH$_2$ppA is a nonhydrolysable compound exerting highly selective postsynaptic action without measurable associated side effects in vivo in *Tsc1*$^{+/-}$ mice suggesting that this compound might constitute a novel therapeutic tool for treatment of different types of epilepsy with a unique highly selective postsynaptic target. Moreover, we have demonstrated that when injected peripherally in the mouse, AppCH$_2$ppA decreases epileptiform activity in the brain in vivo, suggesting that it can cross the blood brain barrier making it a likely candidate as a clinically relevant compound. Future studies will help to clarify further the exact antiepileptic mechanisms of AppCH$_2$ppA and its applicability in clinics.

Supplementary Material

Supplementary material is available at *Cerebral Cortex* online.

Funding

Fondation pour la Recherche Médicale (FDT20170436905) and by Institut National de la Santé et de la Recherche Médicale. A.P.-B. has been a recipient of a MRT (Ministère de la Recherche et de la Technologie) PhD fellowship. M.M. was supported by the subsidy allocated to Kazan University for the state assignment in the sphere of scientific activities (No. 6.2313.2017/4.6). N.B. and A.P.-B. were supported by Fritz Thyssen Stiftung (10.15.2.022MN).

Notes

We thank Svetlana Gataullina for initial pilot in vivo experiments, Morgane Chiesa, Dr Diana C. Ferrari, Pr. Frances Edwards and Dr Yehezkel. Ben-Ari for critically reading the article. A.P.-B. thanks the Fondation pour la Recherche Médicale (FRM) for financial support to this study. A.D.M. thanks the Czech Ministry of Education, Youth and Sports (MŠMT) for OPVVV Project FIT (CZ.02.1.01/0.0/0.0/15_003/0000495) that is financially supported by the European Fund for Regional Development. *Conflict of Interest*: A.D.M. is a shareholder in KP Therapeutics Ltd. that is the current commercial owner of the following patent application; A. D. Miller, N. Lozovaya, N. Burnashev & R. Giniatullin, Dinucleoside polyphosphates for the treatment of epilepsy (compositions), WO2015079241 (A1), 27 November 2013; AU2014356250 (A1); CA2935083 (A1); CN106163561 (A); EP3074042 (A1); JP2017502930 (A); US20163544 02 (A1). The authors are grateful to ImuThes, London, UK, for initial support to carry out preliminary experiments with pharmacologically induced in vitro epilepsy model.

References

Amorim BO, Hamani C, Ferreira E, Miranda MF, Fernandes MJ, Rodrigues AM, de Almeida AC, Covolan L. 2016. Effects of A1 receptor agonist/antagonist on spontaneous seizures in pilocarpine-induced epileptic rats. Epilepsy Behav. 61: 168–173.

Angelatou F, Pagonopoulou O, Maraziotis T, Olivier A, Villemeure JG, Avoli M, Kostopoulos G. 1993. Upregulation of A1 adenosine receptors in human temporal lobe epilepsy: a quantitative autoradiographic study. Neurosci Lett. 163(1): 11–14.

Ault B, Olney MA, Joyner JL, Boyer CE, Notrica MA, Soroko FE, Wang CM. 1987. Pro-convulsant actions of theophylline and caffeine in the hippocampus: implications for the management of temporal lobe epilepsy. Brain Res. 426(1):93–102.

Avoli M, D'Antuono M, Louvel J, Kohling R, Biagini G, Pumain R, D'Arcangelo G, Tancredi V. 2002. Network and pharmacological mechanisms leading to epileptiform synchronization in the limbic system in vitro. Prog Neurobiol. 68(3):167–207.

Baxi MD, Vishwanatha JK. 1995. Diadenosine polyphosphates—their biological and pharmacological significance. J Pharmacol Toxicol Methods. 33(3):121–128.

Boison D. 2005. Adenosine and epilepsy: from therapeutic rationale to new therapeutic strategies. Neuroscientist. 11(1):25–36.

Boison D. 2006. Adenosine kinase, epilepsy and stroke: mechanisms and therapies. Trends Pharmacol Sci. 27(12):652–658.

Boison D. 2012. Adenosine dysfunction in epilepsy. Glia. 60(8): 1234–1243.

Borea PA, Gessi S, Merighi S, Varani K. 2016. Adenosine as a multi-signalling guardian angel in human diseases: when, where and how does it exert its protective effects? Trends Pharmacol Sci. 37(6):419–434.

Brambilla D, Chapman D, Greene R. 2005. Adenosine mediation of presynaptic feedback inhibition of glutamate release. Neuron. 46(2):275–283.

Brundege JM, Dunwiddie TV. 1998. Metabolic regulation of endogenous adenosine release from single neurons. Neuroreport. 9(13):3007–3011.

Ciruela F. 2011. Adenosine receptors. Biochim Biophys Acta. 1808(5):1231–1232.

Cunha RA. 2001. Adenosine as a neuromodulator and as a homeostatic regulator in the nervous system: different roles, different sources and different receptors. Neurochem Int. 38(2):107–125.

Cunha RA, Johansson B, Constantino MD, Sebastiao AM, Fredholm BB. 1996. Evidence for high-affinity binding sites for the adenosine A2A receptor agonist [3H] CGS 21680 in the rat hippocampus and cerebral cortex that are different from striatal A2A receptors. Naunyn Schmiedebergs Arch Pharmacol. 353(3):261–271.

Cunha RA, Sebastiao AM, Ribeiro JA. 1998. Inhibition by ATP of hippocampal synaptic transmission requires localized extracellular catabolism by ecto-nucleotidases into adenosine and channeling to adenosine A1 receptors. J Neurosci. 18(6):1987–1995.

Curatolo P, Bombardieri R, Jozwiak S. 2008. Tuberous sclerosis. Lancet. 372(9639):657–668.

Delaney SM, Blackburn GM, Geiger JD. 1997. Diadenosine polyphosphates inhibit adenosine kinase activity but decrease levels of endogenous adenosine in rat brain. Eur J Pharmacol. 332(1):35–42.

Diaz-Hernandez M, Pereira MF, Pintor J, Cunha RA, Ribeiro JA, Miras-Portugal MT. 2002. Modulation of the rat hippocampal

dinucleotide receptor by adenosine receptor activation. J Pharmacol Exp Ther. 301(2):441–450.

Dunwiddie TV, Diao L, Proctor WR. 1997. Adenine nucleotides undergo rapid, quantitative conversion to adenosine in the extracellular space in rat hippocampus. J Neurosci. 17(20): 7673–7682.

Dunwiddie TV, Masino SA. 2001. The role and regulation of adenosine in the central nervous system. Annu Rev Neurosci. 24:31–55.

El Yacoubi M, Ledent C, Parmentier M, Costentin J, Vaugeois JM. 2008. Evidence for the involvement of the adenosine A(2A) receptor in the lowered susceptibility to pentylenetetrazol-induced seizures produced in mice by long-term treatment with caffeine. Neuropharmacology. 55(1):35–40.

El Yacoubi M, Ledent C, Parmentier M, Costentin J, Vaugeois JM. 2009. Adenosine A2A receptor deficient mice are partially resistant to limbic seizures. Naunyn Schmiedebergs Arch Pharmacol. 380(3):223–232.

Fields RD. 2011. Nonsynaptic and nonvesicular ATP release from neurons and relevance to neuron-glia signaling. Semin Cell Dev Biol. 22(2):214–219.

Fredholm BB, AP IJ, Jacobson KA, Klotz KN, Linden J. 2001. International Union of Pharmacology. XXV. Nomenclature and classification of adenosine receptors. Pharmacol Rev. 53 (4):527–552.

Gataullina S, Lemaire E, Wendling F, Kaminska A, Watrin F, Riquet A, Ville D, Moutard ML, de Saint Martin A, Napuri S, et al. 2016. Epilepsy in young Tsc1(+/–) mice exhibits age-dependent expression that mimics that of human tuberous sclerosis complex. Epilepsia. 57(4):648–659.

Glass M, Faull RL, Bullock JY, Jansen K, Mee EW, Walker EB, Synek BJ, Dragunow M. 1996. Loss of A1 adenosine receptors in human temporal lobe epilepsy. Brain Res. 710(1-2):56–68.

Gouder N, Fritschy JM, Boison D. 2003. Seizure suppression by adenosine A1 receptor activation in a mouse model of pharmacoresistant epilepsy. Epilepsia. 44(7):877–885.

Gouder N, Scheurer L, Fritschy JM, Boison D. 2004. Overexpression of adenosine kinase in epileptic hippocampus contributes to epileptogenesis. J Neurosci. 24(3):692–701.

Haas HL, Selbach O. 2000. Functions of neuronal adenosine receptors. Naunyn Schmiedebergs Arch Pharmacol. 362(4-5): 375–381.

Hargus NJ, Jennings C, Perez-Reyes E, Bertram EH, Patel MK. 2012. Enhanced actions of adenosine in medial entorhinal cortex layer II stellate neurons in temporal lobe epilepsy are mediated via A(1)-receptor activation. Epilepsia. 53(1): 168–176.

Hibino H, Inanobe A, Furutani K, Murakami S, Findlay I, Kurachi Y. 2010. Inwardly rectifying potassium channels: their structure, function, and physiological roles. Physiol Rev. 90(1): 291–366.

Huber A, Padrun V, Deglon N, Aebischer P, Mohler H, Boison D. 2001. Grafts of adenosine-releasing cells suppress seizures in kindling epilepsy. Proc Natl Acad Sci USA. 98(13): 7611–7616.

Jennings LL, Hao C, Cabrita MA, Vickers MF, Baldwin SA, Young JD, Cass CE. 2001. Distinct regional distribution of human equilibrative nucleoside transporter proteins 1 and 2 (hENT1 and hENT2) in the central nervous system. Neuropharmacology. 40(5):722–731.

Klishin A, Lozovaya N, Pintor J, Miras-Portugal MT, Krishtal O. 1994. Possible functional role of diadenosine polyphosphates: negative feedback for excitation in hippocampus. Neuroscience. 58(2):235–236.

Koizumi S, Ohsawa K, Inoue K, Kohsaka S. 2013. Purinergic receptors in microglia: functional modal shifts of microglia mediated by P2 and P1 receptors. Glia. 61(1):47–54.

Kruglikov I, Rudy B. 2008. Perisomatic GABA release and thalamocortical integration onto neocortical excitatory cells are regulated by neuromodulators. Neuron. 58(6):911–924.

Lazarowski ER, Watt WC, Stutts MJ, Boucher RC, Harden TK. 1995. Pharmacological selectivity of the cloned human P2U-purinoceptor: potent activation by diadenosine tetraphosphate. Br J Pharmacol. 116(1):1619–1627.

Leon-Navarro DA, Albasanz JL, Martin M. 2015. Hyperthermia-induced seizures alter adenosine A1 and A2A receptors and 5'-nucleotidase activity in rat cerebral cortex. J Neurochem. 134(3):395–404.

Lesage F, Lazdunski M. 2000. Molecular and functional properties of two-pore-domain potassium channels. Am J Physiol Renal Physiol. 279(5):F793–F801.

Li N, Csepe TA, Hansen BJ, Sul LV, Kalyanasundaram A, Zakharkin SO, Zhao J, Guha A, Van Wagoner DR, Kilic A, et al. 2016. Adenosine-induced atrial fibrillation: localized reentrant drivers in lateral right atria due to heterogeneous expression of adenosine A1 receptors and GIRK4 subunits in the human heart. Circulation. 134(6):486–498.

Lim JS, Gopalappa R, Kim SH, Ramakrishna S, Lee M, Kim WI, Kim J, Park SM, Lee J, Oh JH, et al. 2017. Somatic mutations in TSC1 and TSC2 cause focal cortical dysplasia. Am J Hum Genet. 100(3):454–472.

Lim JS, Kim WI, Kang HC, Kim SH, Park AH, Park EK, Cho YW, Kim S, Kim HM, Kim JA, et al. 2015. Brain somatic mutations in MTOR cause focal cortical dysplasia type II leading to intractable epilepsy. Nat Med. 21(4):395–400.

Lopes LV, Cunha RA, Ribeiro JA. 1999. Cross talk between A(1) and A(2A) adenosine receptors in the hippocampus and cortex of young adult and old rats. J Neurophysiol. 82(6):3196–3203.

Lopes LV, Halldner L, Rebola N, Johansson B, Ledent C, Chen JF, Fredholm BB, Cunha RA. 2004. Binding of the prototypical adenosine A(2A) receptor agonist CGS 21680 to the cerebral cortex of adenosine A(1) and A(2A) receptor knockout mice. Br J Pharmacol. 141(6):1006–1014.

Lovatt D, Xu Q, Liu W, Takano T, Smith NA, Schnermann J, Tieu K, Nedergaard M. 2012. Neuronal adenosine release, and not astrocytic ATP release, mediates feedback inhibition of excitatory activity. Proc Natl Acad Sci USA. 109(16):6265–6270.

Lozovaya N, Gataullina S, Tsintsadze T, Tsintsadze V, Pallesi-Pocachard E, Minlebaev M, Goriounova NA, Buhler E, Watrin F, Shityakov S, et al. 2014. Selective suppression of excessive GluN2C expression rescues early epilepsy in a tuberous sclerosis murine model. Nature Communications. 5:4563.

Marchi M, Raiteri L, Risso F, Vallarino A, Bonfanti A, Monopoli A, Ongini E, Raiteri M. 2002. Effects of adenosine A1 and A2A receptor activation on the evoked release of glutamate from rat cerebrocortical synaptosomes. Br J Pharmacol. 136(3): 434–440.

Marsan E, Baulac S. 2018. Review: mechanistic target of rapamycin (mTOR) pathway, focal cortical dysplasia and epilepsy. Neuropathol Appl Neurobiol. 44(1):6–17.

Mathew SS, Pozzo-Miller L, Hablitz JJ. 2008. Kainate modulates presynaptic GABA release from two vesicle pools. J Neurosci. 28(3):725–731.

Mathie A, Al-Moubarak E, Veale EL. 2010. Gating of two pore domain potassium channels. J Physiol. 588(Pt 17):3149–3156.

Melnik S, Wright M, Tanner JA, Tsintsadze T, Tsintsadze V, Miller AD, Lozovaya N. 2006. Diadenosine polyphosphate analog controls postsynaptic excitation in CA3-CA1

synapses via a nitric oxide-dependent mechanism. J Pharmacol Exp Ther. 318(2):579–588.
Meng XF, Yu JT, Song JH, Chi S, Tan L. 2013. Role of the mTOR signaling pathway in epilepsy. J Neurol Sci. 332(1-2):4–15.
Miras-Portugal MT, Gualix J, Mateo J, Diaz-Hernandez M, Gomez-Villafuertes R, Castro E, Pintor J. 1999. Diadenosine polyphosphates, extracellular function and catabolism. Prog Brain Res. 120:397–409.
Moller RS, Weckhuysen S, Chipaux M, Marsan E, Taly V, Bebin EM, Hiatt SM, Prokop JW, Bowling KM, Mei D, et al. 2016. Germline and somatic mutations in the MTOR gene in focal cortical dysplasia and epilepsy. Neurol Genet. 2(6):e118.
Mustafa SJ, Morrison RR, Teng B, Pelleg A. 2009. Adenosine receptors and the heart: role in regulation of coronary blood flow and cardiac electrophysiology. Handb Exp Pharmacol. 193:161–188.
Newby AC. 1986. How does dipyridamole elevate extracellular adenosine concentration? Predictions from a three-compartment model of adenosine formation and inactivation. Biochem J. 237(3):845–851.
Pagonopoulou O, Efthimiadou A, Asimakopoulos B, Nikolettos NK. 2006. Modulatory role of adenosine and its receptors in epilepsy: possible therapeutic approaches. Neurosci Res. 56 (1):14–20.
Pintor J, Diaz-Rey MA, Miras-Portugal MT. 1993. Ap4A and ADP-beta-S binding to P2 purinoceptors present on rat brain synaptic terminals. Br J Pharmacol. 108(4):1094–1099.
Pintor J, King BF, Miras-Portugal MT, Burnstock G. 1996. Selectivity and activity of adenine dinucleotides at recombinant P2X2 and P2Y1 purinoceptors. Br J Pharmacol. 119(5):1006–1012.
Pintor J, Miras-Portugal MT. 1995. P2 purinergic receptors for diadenosine polyphosphates in the nervous system. Gen Pharmacol. 26(2):229–235.
Punke MA, Licher T, Pongs O, Friederich P. 2003. Inhibition of human TREK-1 channels by bupivacaine. Anesth Analg. 96 (6):1665–1673. table of contents.
Rebola N, Coelho JE, Costenla AR, Lopes LV, Parada A, Oliveira CR, Soares-da-Silva P, de Mendonca A, Cunha RA. 2003. Decrease of adenosine A1 receptor density and of adenosine neuromodulation in the hippocampus of kindled rats. Eur J Neurosci. 18(4):820–828.
Reddy DS, Kuruba R. 2013. Experimental models of status epilepticus and neuronal injury for evaluation of therapeutic interventions. Int J Mol Sci. 14(9):18284–18318.
Rodrigues RJ, Tome A, Cunha RA. 2015. ATP as a multi-target danger signal in the brain. Front Neurosci. 9:148.
Rotermund N, Winandy S, Fischer T, Schulz K, Fregin T, Alstedt N, Buchta M, Bartels J, Carlstrom M, Lohr C, et al. 2018. Adenosine A1 receptor activates background potassium channels and modulates information processing in olfactory bulb mitral cells. J Physiol. 596(4):717–733.
Rubino A, Burnstock G. 1996. Possible role of diadenosine polyphosphates as modulators of cardiac sensory-motor neurotransmission in guinea-pigs. J Physiol. 495(Pt 2):515–523.
Schachter JB, Li Q, Boyer JL, Nicholas RA, Harden TK. 1996. Second messenger cascade specificity and pharmacological selectivity of the human P2Y1-purinoceptor. Br J Pharmacol. 118(1):167–173.
Schmidt D, Schachter SC. 2014. Drug treatment of epilepsy in adults. Br Med J. 348:g254.
Sharma AK, Rani E, Waheed A, Rajput SK. 2015. Pharmacoresistant epilepsy: a current update on non-conventional pharmacological and non-pharmacological interventions. J Epilepsy Res. 5(1):1–8.
Shin HW, Soh JS, Kim HZ, Hong J, Woo DH, Heo JY, Hwang EM, Park JY, Lee CJ. 2014. The inhibitory effects of bupivacaine, levobupivacaine, and ropivacaine on K2P (two-pore domain potassium) channel TREK-1. J Anesth. 28(1):81–86.
Siggins GR, Schubert P. 1981. Adenosine depression of hippocampal neurons in vitro: an intracellular study of dose-dependent actions on synaptic and membrane potentials. Neurosci Lett. 23(1):55–60.
Sodickson DL, Bean BP. 1998. Neurotransmitter activation of inwardly rectifying potassium current in dissociated hippocampal CA3 neurons: interactions among multiple receptors. J Neurosci. 18(20):8153–8162.
Studer FE, Fedele DE, Marowsky A, Schwerdel C, Wernli K, Vogt K, Fritschy JM, Boison D. 2006. Shift of adenosine kinase expression from neurons to astrocytes during postnatal development suggests dual functionality of the enzyme. Neuroscience. 142(1):125–137.
Takigawa T, Alzheimer C. 1999. G protein-activated inwardly rectifying K+ (GIRK) currents in dendrites of rat neocortical pyramidal cells. J Physiol. 517(Pt 2):385–390.
Trussell LO, Jackson MB. 1985. Adenosine-activated potassium conductance in cultured striatal neurons. Proc Natl Acad Sci USA. 82(14):4857–4861.
Tupone D, Madden CJ, Morrison SF. 2013. Central activation of the A1 adenosine receptor (A1AR) induces a hypothermic, torpor-like state in the rat. J Neurosci. 33(36): 14512–14525.
van Aerde KI, Qi G, Feldmeyer D. 2015. Cell type-specific effects of adenosine on cortical neurons. Cereb Cortex. 25(3): 772–787.
Wall MJ, Atterbury A, Dale N. 2007. Control of basal extracellular adenosine concentration in rat cerebellum. J Physiol. 582 (Pt 1):137–151.
Wall M, Dale N. 2008. Activity-dependent release of adenosine: a critical re-evaluation of mechanism. Curr Neuropharmacol. 6(4):329–337.
Wall MJ, Richardson MJE. 2015. Localized adenosine signaling provides fine-tuned negative feedback over a wide dynamic range of neocortical network activities. J Neurophysiol. 113 (3):871–882.
Ward JL, Sherali A, Mo ZP, Tse CM. 2000. Kinetic and pharmacological properties of cloned human equilibrative nucleoside transporters, ENT1 and ENT2, stably expressed in nucleoside transporter-deficient PK15 cells. Ent2 exhibits a low affinity for guanosine and cytidine but a high affinity for inosine. J Biol Chem. 275(12):8375–8381.
Wildman SS, Brown SG, King BF, Burnstock G. 1999. Selectivity of diadenosine polyphosphates for rat P2X receptor subunits. Eur J Pharmacol. 367(1):119–123.
Yamada M, Inanobe A, Kurachi Y. 1998. G protein regulation of potassium ion channels. Pharmacol Rev. 50(4):723–760.
Yamashiro K, Morita M. 2017. Novel aspects of extracellular adenosine dynamics revealed by adenosine sensor cells. Neural Regen Res. 12(6):881–885.
Zeng LH, Rensing NR, Wong M. 2009. The mammalian target of rapamycin signaling pathway mediates epileptogenesis in a model of temporal lobe epilepsy. J Neurosci. 29(21): 6964–6972.
Zhang P, Bannon NM, Ilin V, Volgushev M, Chistiakova M. 2015. Adenosine effects on inhibitory synaptic transmission and excitation-inhibition balance in the rat neocortex. J Physiol. 593(4):825–841.